AD-A076 586 RCA GOVERNMENT SYSTEMS DIV BURLINGTON MA F/G 19/5
RADAR TARGETING TECHNIQUE, REPORT OF METHODS AND RESULTS.(U)
NOV 79 J M ANDERSON , E L WIRTZ DAAB07-78-C-3613
UNCLASSIFIED DELEW-TR-78-3613-F NL

1 OF 2
AD
A076586


D
076586
1.0
1.1
1.25
1.4
1.6
2.8
3.2
3.6
4.0
2.5
2.2
2.0
1.8
MICROCOPY RESOLUTION TEST CHART
NATIONAL BUREAU OF STANDARDS-1963-A

LEVEL II

Research and Development Technical Report

DELEW-TR-78-3613-F

RADAR TARGETING TECHNIQUE REPORT OF METHODS AND RESULTS

J.M. Anderson and E.L. Wirtz
RCA CORPORATION
Government Systems Division
Burlington, MA 01803

November 1979

Final Report for Period 5 July 1978 - 30 June 1979

DISTRIBUTION STATEMENT

Approved for public release;
distribution unlimited

Prepared for
Defense Advanced Research Projects Agency
1400 Wilson Blvd.
Arlington, VA 22209

ERADCOM

US ARMY ELECTRONICS RESEARCH AND DEVELOPMENT COMMAND
FORT MONMOUTH, NEW JERSEY 07703

NOTICES

Disclaimers

The citation of trade names and names of manufacturers in this report is not to be construed as official Government indorsement or approval of commercial products or services referenced herein.

Disposition

Destroy this report when it is no longer needed. Do not return it to the originator.

SECURITY CLASSIFICATION OF THIS PAGE (When Data Entered)

(19) REPORT DOCUMENTATION PAGE		READ INSTRUCTIONS BEFORE COMPLETING FORM
(18) 1. REPORT NUMBER DELEW-TR-78-3613-F	2. GOVT ACCESSION NO.	3. RECIPIENT'S CATALOG NUMBER
(6) 4. TITLE (and Subtitle) Radar Targeting Technique, Report of Methods & Results, and		5. TYPE OF REPORT & PERIOD COVERED Final Report 07-05-78 thru 06-30-79
		6. PERFORMING ORG. REPORT NUMBER
(10) 7. AUTHOR(s) J.M. Anderson E.L. Wirtz		(15) 8. CONTRACT OR GRANT NUMBER(s) DAAB07-78-C-3613
9. PERFORMING ORGANIZATION NAME AND ADDRESS RCA Corporation Government Systems Div., Box 588 Burlington, MA 01803 410 699		10. PROGRAM ELEMENT, PROJECT, TASK AREA & WORK UNIT NUMBERS 3.10.11.G (12) 94
11. CONTROLLING OFFICE NAME AND ADDRESS Commander, US Army Electronics R&D Command ATTN: DELEW-E Ft. Monmouth, NJ 07703		12. REPORT DATE (11) Nov 79
		13. NUMBER OF PAGES 82
14. MONITORING AGENCY NAME & ADDRESS (if different from Controlling Office) Defense Advanced Research Projects Agency 1400 Wilson Blvd. Arlington, VA 22209		15. SECURITY CLASS. (of this report) UNCLASSIFIED
		15a. DECLASSIFICATION/DOWNGRADING SCHEDULE

16. DISTRIBUTION STATEMENT (of this Report)

Distribution is unlimited. Approved for public release.

17. DISTRIBUTION STATEMENT (of the abstract entered in Block 20, if different from Report)

(9) Final rept. 5 Jul 78-30 Jun 79,

18. SUPPLEMENTARY NOTES

19. KEY WORDS (Continue on reverse side if necessary and identify by block number)

Expendable, Repeater, ELINT, Radar, Time of Arrival (TOA), Targeting, Direction Finding (DF), Difference in Time of Arrival (DTOA)

20. ABSTRACT (Continue on reverse side if necessary and identify by block number)

A specific radar targeting technique, using a collection station and a single microwave repeater to acquire targeting quality location information on radar emitters, was successfully examined and tested. The concept implements a combination of microwave direction finding (DF) and difference in time-of-arrival (DTOA) processes. Analytical results suggest that, at victim radar ranges of 15 km, location accuracies of the order of tens of meters are achievable.

DD FORM 1 JAN 73 1473 EDITION OF 1 NOV 65 IS OBSOLETE

410 699

SECURITY CLASSIFICATION OF THIS PAGE (When Data Entered)

TABLE OF CONTENTS

TABLE OF CONTENTS (Cont.)

LIST OF ILLUSTRATIONS

LIST OF ILLUSTRATIONS (Cont.)

LIST OF TABLES

ABBREVIATIONS

BS	base station
DF	direction finding
DOA	direction of arrival
DTOA	difference in time of arrival
ECCM	electronic counter-countermeasures
ECM	electronic countermeasures
ELINT	electronic intelligence
ERP	effective radiated power
EXPELS	expendable precision emitter locator system
FEBA	forward edge of the battle area
GFE	government-furnished equipment
IF	intermediate frequency
LC	location code
LOS	line of sight
R	repeater
RF	radio frequency
RMS	root mean squared
RPV	remotely piloted vehicle
RSS	root sum squared
RTT	radar targeting technique
S/N	signal to noise
TOA	Time of arrival
V	victim
VSWR	voltage standing wave ratio

SECTION 1

SECTION 1
INTRODUCTION AND SUMMARY

In the forward edge of battle area, a key problem in neutralizing enemy firepower is the location of his weapon system emitters with sufficient precision for targeting.

The Radar Targeting Technique I (RTT-1) concept involves the use of a single ELINT base station and a single microwave repeater to locate victim radars with targeting precision. It accomplishes this by means of a combination of DF measurements at the base station and TOA and DTOA measurements between the base station and repeater.

This program, Contract No. DAAB07-78-C-3613, was jointly sponsored by DARPA and the U.S. Army ERADCOM EW Laboratory. Its objective was to assess the technical feasibility of the RTT-1 concept. Specifically, it was desired to ascertain the impact of multipath and foliage and terrain obstructions on the system when operated in the field in conjunction with radiation from the minor lobes of a victim radar's antenna.

To accomplish this objective, an RTT-1 test system was assembled at RCA in Burlington, Massachusetts and tested at the Wayside Test Area, U.S. Naval Ammunition Depot, Earle, New Jersey, during June 1979. Tests were conducted on a reduced-scale test range and the results extrapolated to conform to an approximate 15 kilometer range operation.

It was found that the dominant error in the RTT-1 test system was multipath from diffuse scatters. The effects, however, were statistically well-behaved and did not significantly impact overall system target location performance.

Foliage and terrain obstruction effects were encountered and determined to be analytically predictable. These effects, in the worst case, can render an RTT-1 system inoperable. In general, however, expected obstruction characteristics can be used to establish RTT-1 design requirements which should permit substantial operational flexibility.

Specular multipath effects were determined to be the most serious system problem. Their impact can be mitigated by the use of directive antennas in the RTT-1 base station, first-pulse only time measurement techniques, and ancillary operator displays to recognize their presence.

The results of this technical feasibility assessment are sufficiently promising to warrant additional attention being paid the RTT-1 concept or variants thereof. These include:

1. Use of an RPV-borne repeater to operate in conjunction with such U.S. Army ground based ELINT assets as the AN/MSQ-103.
2. Use of surface-located repeaters to permit closed-loop missile guidance toward victim emitters.
3. Use of an operational version of the RTT-1 test system in regions where terrain irregularity and foliage conditions permit.

An appropriate early "next step" is the evaluation of a helicopter-borne version of the RTT-1 repeater against a simulated threat radar.

SECTION 2

SECTION 2
STATEMENT OF PROBLEM

The radar targeting technique being examined under this program implements a concept in which an ELINT base station and a single microwave repeater are employed to acquire targeting-quality location information on radar emitters. A combination of microwave direction-finding and difference in time-of-arrival processes are employed. Analytical results suggest that, at a victim radar range of 15 kilometers, location accuracies of the order of tens of meters should be achievable as measured at the base station.

The analytical results alone are not considered adequate to support developmental attention. They do not account for the multipath-produced performance degradation historically observed in systems employing similar processes, nor do they satisfactorily treat over-the-horizon or foliage penetration propagation path situations. The problem being addressed in this program, then, is assessment of the technical feasibility of the radar targeting technique.

2-1. CONCEPT DESCRIPTION

The radar targeting technique, designated RTT-1, is intended for use in acquiring the location of victim radars in the vicinity of the forward edge of the battle area (FEBA) in order to bring weapon fire against them. As shown in Figure 2-1, the RTT-1 technique uses two functional elements: an unattended microwave repeater and a vehicle-mounted base station.

The functions of the repeater are to:

- Provide a known point in hostile territory (in principle, the base station and the repeater form a two-station difference-in-time of arrival baseline)
- Relay emissions from the victim emitter to the base station.

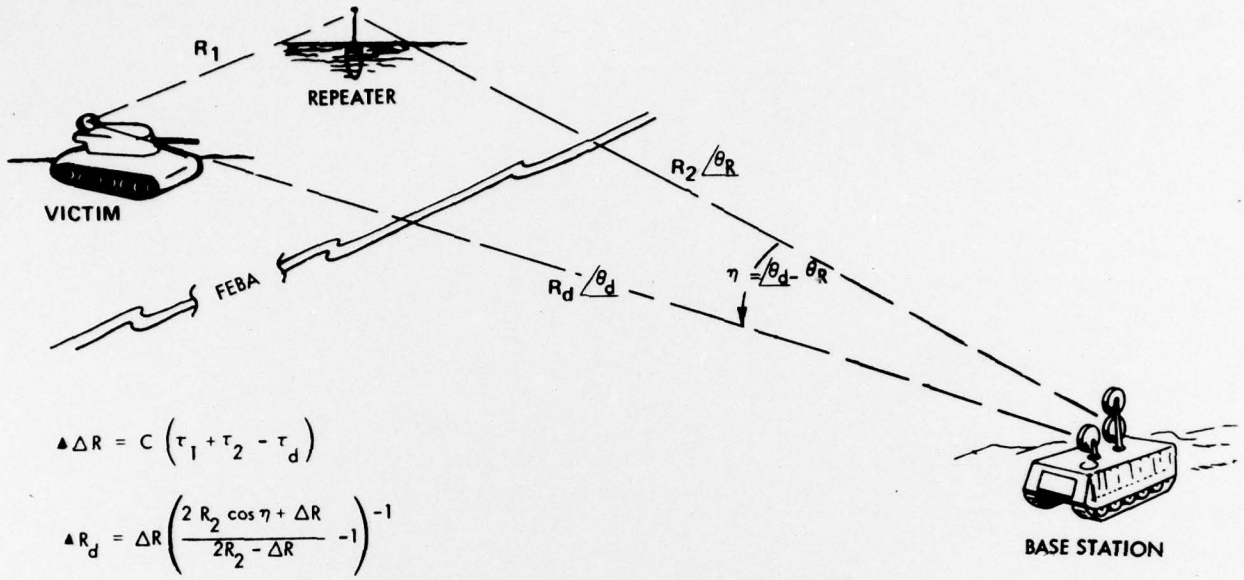

Figure 2-1. RTT-1 Concept

The functions of the base station are to:

- Detect and identify the enemy emitter and obtain a line of bearing to it
- Interrogate the repeater and measure range and bearing to it
- Measure the difference in time-of-arrival between direct path and repeated emissions
- Determine the precise location of the victim emitter and communicate that information to an appropriate weapon.

The range to the victim radar may be computed from the expression:

$$R_d = C\tau_d\left(\frac{2\tau_2 \cos\eta + \tau_d}{2\tau_2 - \tau_d} - 1\right)^{-1} \qquad (2\text{-}1)$$

where:

R_d = base station to victim emitter range.

C = velocity of microwave propogation in the earth's atmosphere (2.997×10^8 meters/second).

τ_d = measured difference in time-of-arrival between direct path and repeated path emissions.

τ_2 = one-half of measured difference in time between transmission of interrogate pulse to repeater and receipt of response pulse from the repeater as measured at the base station.

$\eta = \theta_d - \theta_R$ = planar angle between line of bearing from base station to the victim radar (θ_d) and line of bearing to the repeater (θ_R).

The range error standard deviation (i.e., that encountered in determining R_d), is given by:

$$\sigma(R_d) = \frac{2R_d^2}{\Delta R^2 (2R_2 - \Delta R)^2} \left\{ [(\Delta R)^2 + 2R_2 (1 - \cos\eta)(R_2 - \Delta R)]^2 \sigma_{\Delta R}^2 \right.$$

$$\left. + (\Delta R)^4 (1 + \cos\eta)^2 \sigma_{R_2}^2 + [\Delta R(2R_2 - \Delta R) R_2 \sin\eta]^2 \sigma_\eta^2 \right\}^{1/2} \quad (2\text{-}2)$$

where:

R_d, R_2, η are as indicated in Figure 2-1.

$\sigma_{R_2} = C\sigma_{\tau_d}$

$\sigma_{\Delta R} = C\sigma_{\tau_d}$

$\sigma_\eta, \sigma_{\tau_2}, \sigma_{\tau_d}$ are parameter measurement standard deviations.

The deflection error standard deviation is given by:

$$\sigma_{R\ (DEFL)} = R_d \sigma_{\theta_d} \qquad (2\text{-}3)$$

where:

$\sigma_{\theta d}$ is the bearing measurement standard deviation associated with the victim radar DF cut.

The location error associated with the RTT-1 technique has the geometry indicated in Figure 2-2. It is seen to be an approximate parallelogram generated by lines bounding the uncertainty in the base station's ability to DF on the victim radar, and lines bounding the location uncertainty associated with the DTOA measurement. As expected, a geometric dilution of precision (GEDOP) exists which is determined by the relative locations of the base station, the victim radar and the expendable repeater. Accuracy contours describing the predicted GEDOP are shown in Figure 2-3. These are consistent with:

1. 15 kilometer base station to victim radar range
2. Flat earth
3. The region of expendable repeater deployment shown on these coordinates of the graph,
4. The system parameters identified in the figure.

If it is assumed that the maximum tolerable range error is 40 meters, then the region of permissible repeater location will be as indicated by the shaded area in Figure 2-2. If the DTOA, TOA and DF standard deviation factors are greater than the 3.35 μseconds and 0.25^{o} assumed, then the 40 meter accuracy contour will tend the close toward the ordinate axis, i.e., toward where the 20 meter accuracy contour presently lies, for instance.

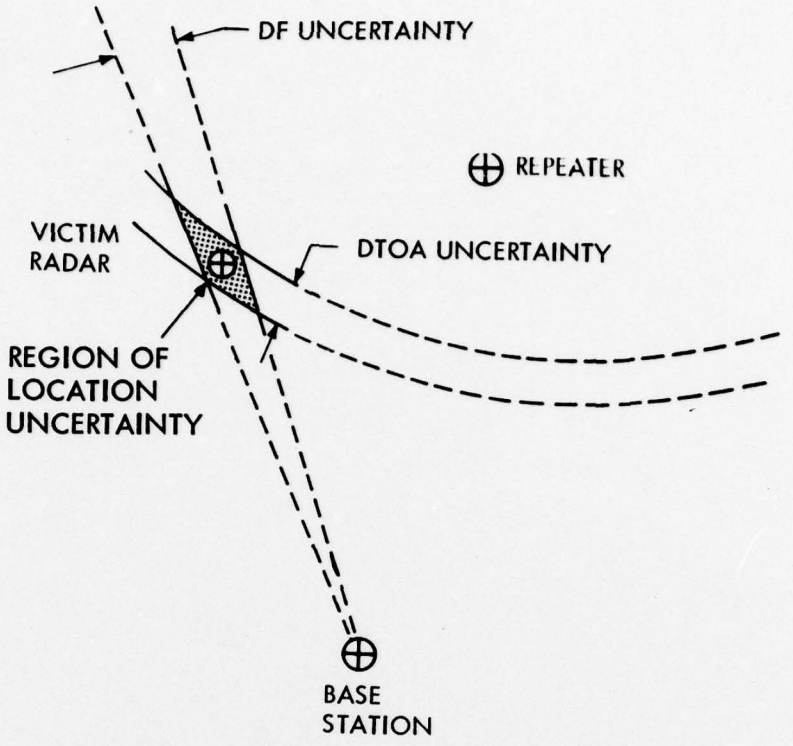

Figure 2-2. RTT-1 Location Error Geometry

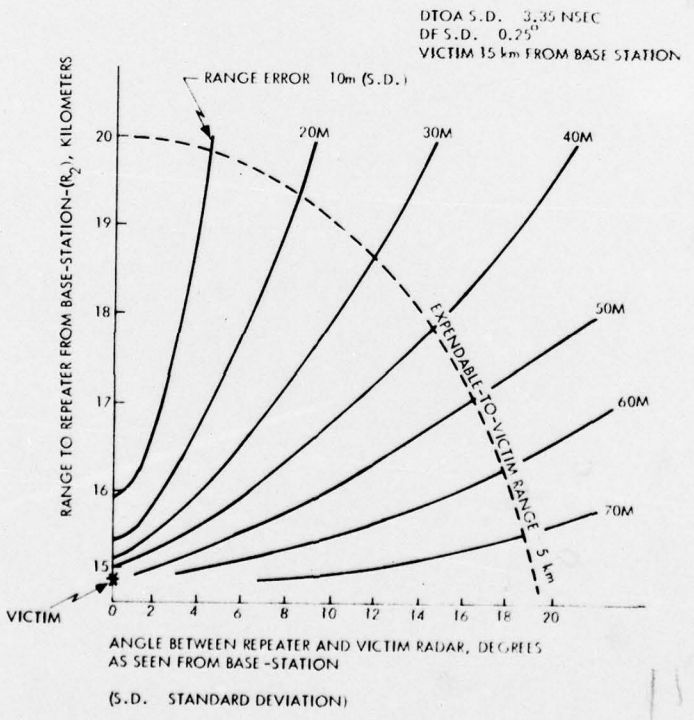

Figure 2-3. RTT-1 Accuracy Contours

2.2 TECHNICAL FEASIBILITY UNCERTAINTY

Technical uncertainty regarding RTT-1 feasibility centers on the potential impact of ground-ground propagation phenomena upon TOA, DTOA and DF measurement capability. Pulse shape distortion due to multipath in the victim radar to repeater link can be expected to result in large TOA and DTOA errors (e.g., approaching $\pm$100 ns). Foliage interruption of link line-of-sight paths will introduce both signal attenuation (degrading link signal to noise performance) and pulse shape distortion (degrading DTOA measurement accuracy). Terrain obstructions will produce similar effects.

The effects of these factors on system operation would, of course, depend on their severity. The impact could go so far as to make operation impossible; or, more probably, it could reduce the region of repeater deployment to critically small dimensions. Since the factors are very situation-dependent and difficult to examine analytically, experimental evidence is necessary to evaluate their impact on system performance.

SECTION 3

SECTION 3
TECHNICAL FEASIBILITY ASSESSMENT

Assessing the technical feasibility of the RTT-1 concept requires a determination of:

1. Adequacy of the analytical model

   - Have all salient variables been accounted for?
   - Is operation predictable?

2. Adequacy of the present state-of-the-art to support operationally meaningful performance objectives.

   - Are the requisite bearing measurement and time-of-arrival measurement accuracies achievable?
   - What system margins are available?

3.1 FEASIBILITY ASSESSMENT APPROACH

Adequacy of the RTT-1 analytical model was determined by operating the essential system elements (base station and repeater) against a simulated threat radar at surveyed test locations in the Wayside Test Area at Fort Monmouth, New Jersey. Due to range size limitations, path length scaling was practiced. Situation geometry consistent with 15-kilometer base station to victim radar range was used. Similarly, link S/N ratios were kept consistent with a 15-kilometer base station to victim range by using appropriate RF attenuators in each link.

Data was collected to permit examination of the impact of propagation effects upon TOA, DTOA and DF measurements, and to compute the location of the victim radar. The latter was directly compared with surveyed location data to identify the location error. The location errors were, in turn, compared with predicted geometric dilution of precision contours to identify any deviation of the test system performance from that analytically predicted.

Test situations were selected to permit separate examination of the effects of multipath, foliage and terrain obstructions upon test system operation.

Adequacy of the state-of-the-art to support meaningful performance objectives was determined by examination of the upgraded (by the test results) analytical model.

3.2 TEST SYSTEM DESCRIPTION

3.2.1 General

The test system configuration used for RTT-1 feasibility assessment is shown in the block diagram of Figure 3-1. A combination of laboratory test equipment, breadboard equipment and GFE were used.

An AN/PPS-5 radar was used both as the victim radar during DTOA measurements and (operated with the base station microwave antenna) as the base station interrogator during repeater TOA measurements. Though cumbersome, this practice permitted accurate sorting of the impact of victim-repeater multipath effects from other sources of measurement error. A photograph of the AN/PPS-5 radar as deployed for operation as the victim radar is shown in Figure 3-2.

An RCA repeater, used during the tests, is shown in Figure 3-3. A heterodyne implementation employing a Class C output power amplifier was used to convert received K-band pulses from the AN/PPS-5 into L-band pulses for retransmission to the base station.

The base station, configured to function as an interrogator, is shown in Figure 3-4. The AN/PPS-5 transmitter is seen mounted behind the antenna pedestal, midway between the upper K-band and lower L-band reflectors.

Figure 3-5 depicts the base station, configured for DTOA measurement. The operator on the left is using the theodolite for direct observation of the victim radar. This was done to permit examination of DF measurement errors.

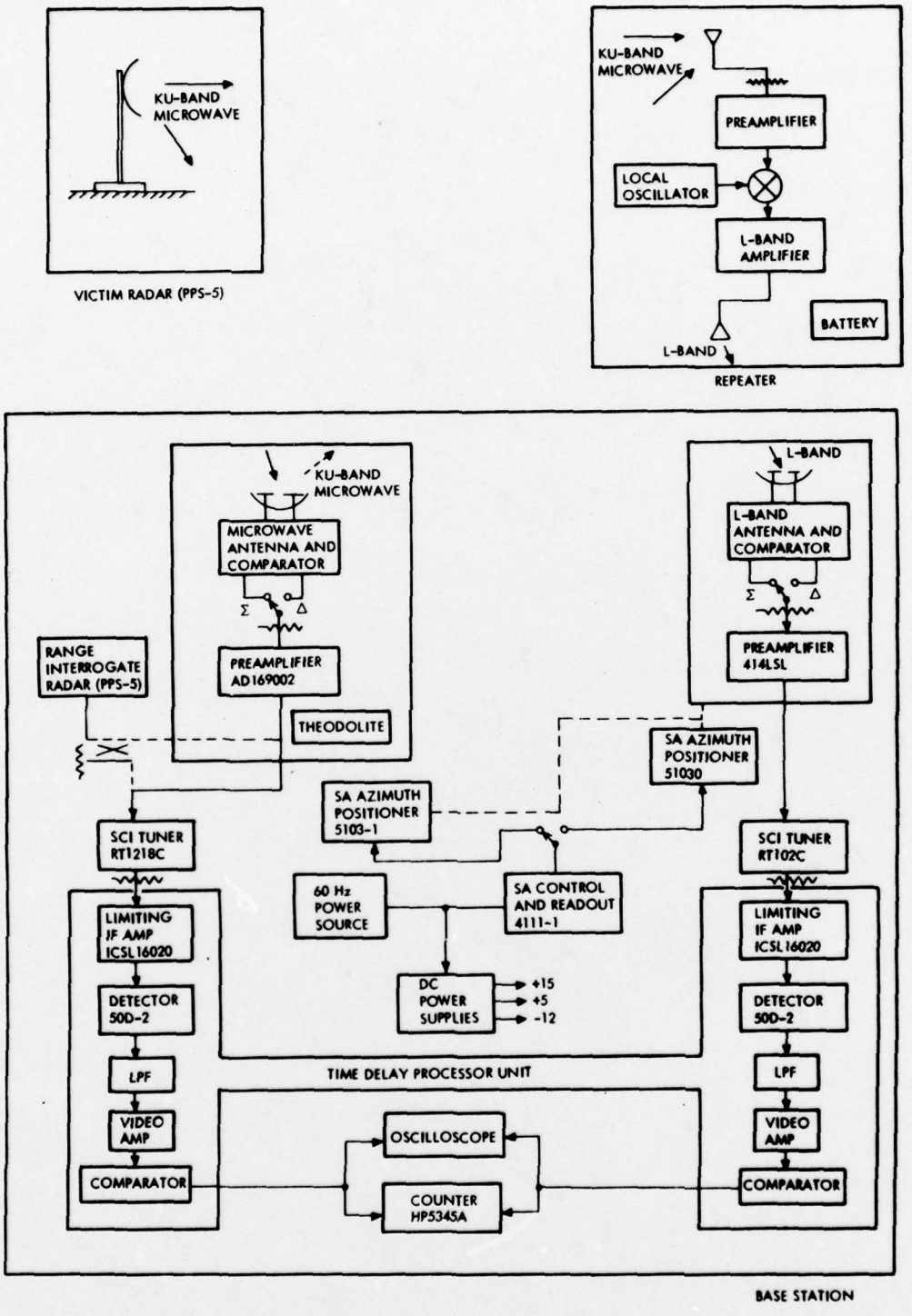

Figure 3-1. RTT-1 Test Configuration

Figure 3-2. AN/PPS-5 Radar

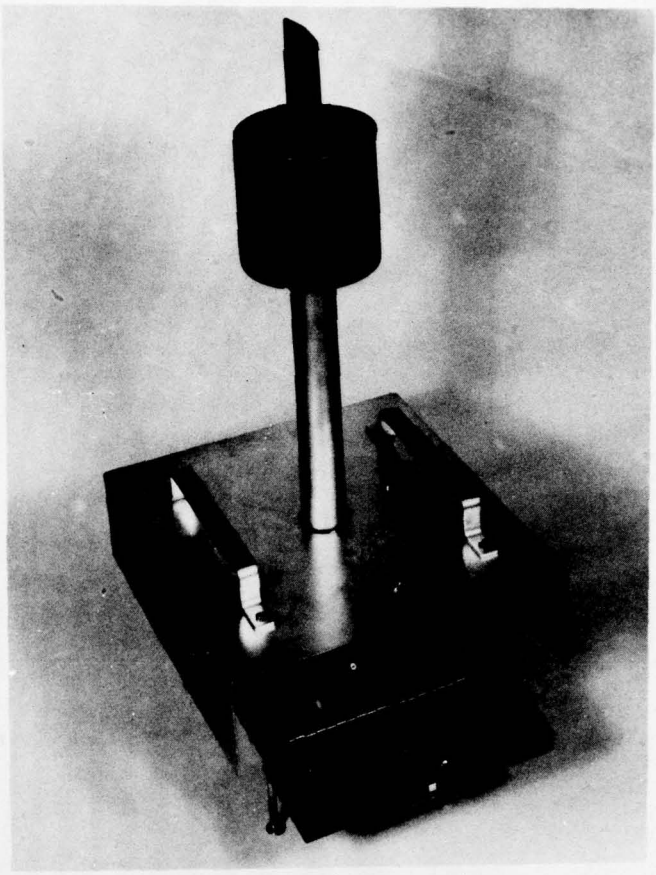

Figure 3-3. Breadboard Repeater with Control Panel Exposed

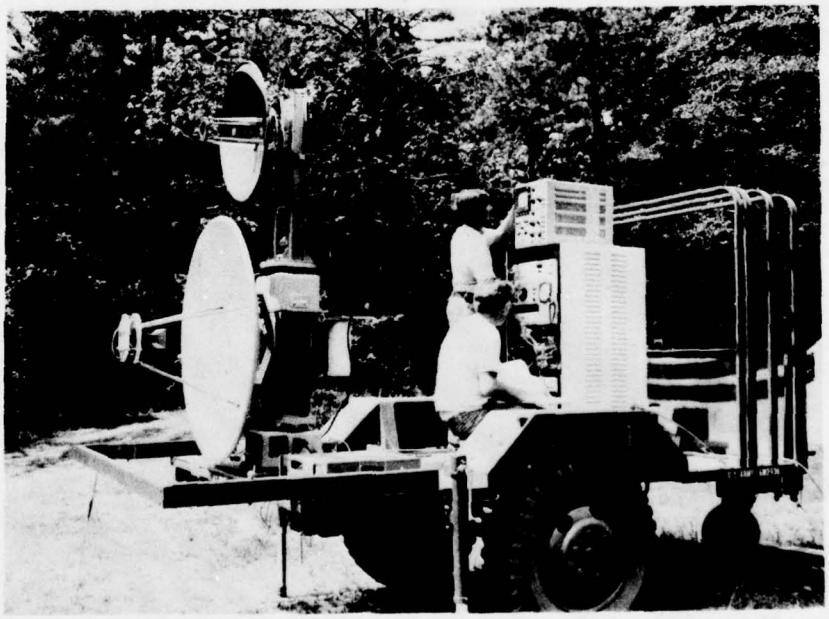

Figure 3-4. Base Station Configured to Function as an Interrogator

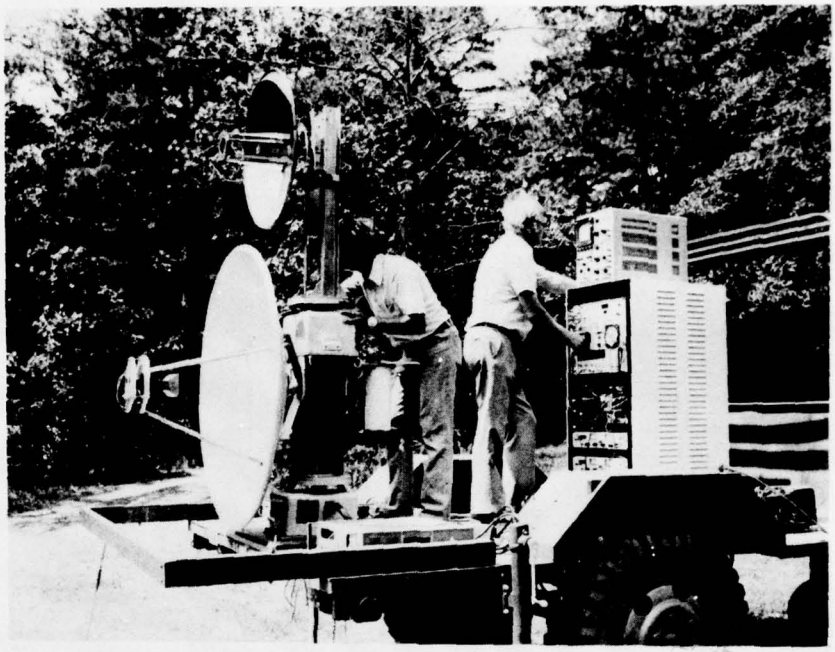

Figure 3-5. Base Station Configured for DTOA Measurement

Monopulse DF instrumentation was used for both receiver channels. Identical components were used in both base station receivers to assure equal time delay in both cases. Microwave and RF cable lengths were made equal to minimize the bias in DTOA measurements.

A concentric mounting arrangement for the two receiving antenna systems was used, with two azimuth positioners. Concentric mounting, as applied here, eliminates any parallaz problem and the requirement for precision angle readout of both positioners. The microwave antenna and theodolite are mounted on the upper positioner, which in turn rests on top of the L-Band antenna positioner. The bottom positioner must be capable of vernier adjustment, but accurate precision readout of it is not required.

Boresighting was accomplished by colocation (or location along a constant bearing) of the repeater and the victim radar.

The AN/PPS-5 transmitter was used to perform the interrogate function as shown in Figure 3-1. As indicated, an attenuated sample of the transmitted pulse provided a timing reference for the TOA ranging measurements.

Detailed descriptions of the test equipment follow in paragraph 3.2.2.

3.2.2 Test Equipment

3.2.2.1 Victim Radar (AN/PPS-5) - The AN/PPS-5 victim radar has the following specified characteristics:

Victim Radar (PPS-5)

Frequency (Tunable)	16.0 - 16.25 GHz
Peak Power	1 kW (+60 dBm)
Average Power	1 Watt (+30 dBm)
Pulse Repetition Rate	4000 pps ± 5%
Pulse Width	0.25 usec
Antenna - Axial Bandwidth	1.125 (3 dB)
- Elevation Bandwidth	3.48° (3 dB)
- Sidelobe/Backlobe	17 dB Down
- Polarization	Horizontal

Assuming 80% radiation efficiency, the main lobe ERP is then:

$$+ 60 \text{ dB} + 39.2 \text{ dB} = + 99.2 \text{ dBm}$$

The sidelobe/backlobe ERP was determined to be approximately:

$$+ 99.2 - 17 = + 82.2 \text{ dBm}$$

Laboratory measurements on the transmitter output were made prior to the field test deployment and included detected RF pulse shape, transmit spectrum shape, peak output power, and frequency tuning range. Figures 3-6 and 3-7 show photographs of the detected RF pulse and spectrum, respectively. The measured peak power output was slightly greater than +60 dBm with a magnetron tuning range of 16.0 - 16.25 GHz.

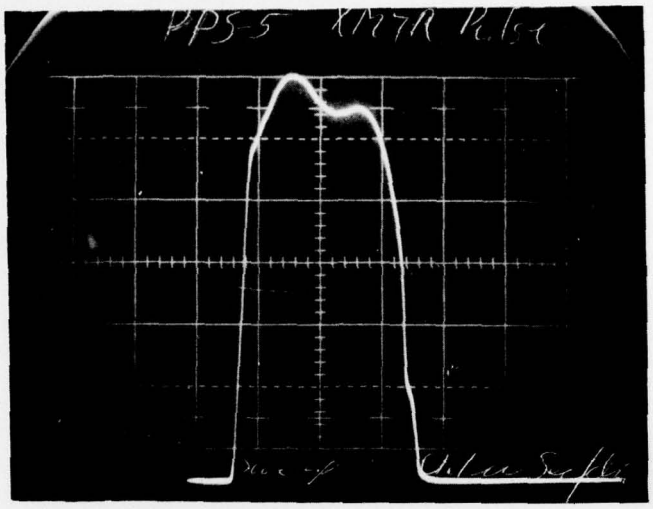

0.1 μsec/cm

Figure 3-6. Detected RF Pulse Showing Rise Time and Pulse Width

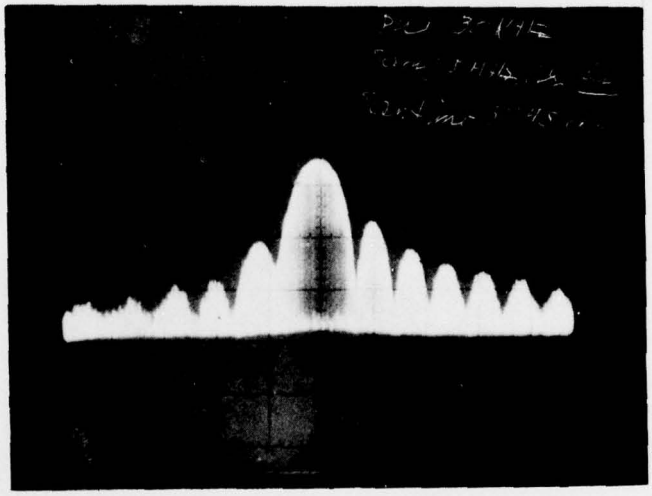

10 dB/Div

5 MHz/Div

Figure 3-7. Transmitted Spectrum Amplitude Characteristic

During the field tests, the AN/PPS-5 antenna was operated in the stationary mode (non-scanning) and pointed 180 degrees with respect to the line bisecting the angle formed by the repeater, victim radar and base station location.

3.2.2.2 Interrogate Radar - As shown in Figure 3-1, an AN/PPS-5 transmitter was also used to perform the interrogate radar function in conjunction with the base station microwave antenna (sum channel). Measured gain of the transmit antenna (see Paragraph 3.2.2.4) was 30.4 dB, resulting in an ERP of +90.4 dBm. A 70 dB RF coupler was used to obtain a reference channel signal at a level of -10 dBm, inserted at the microwave receiver input.

3.2.2.3 Repeater - Figures 3-8 and 3-9 show respectively a block diagram and schematic diagram for the heterodyne repeater.

A photograph of the unit was shown in Figure 3-3. An offset shield with a highly reflective surface is included to limit the effect of absorption of direct solar

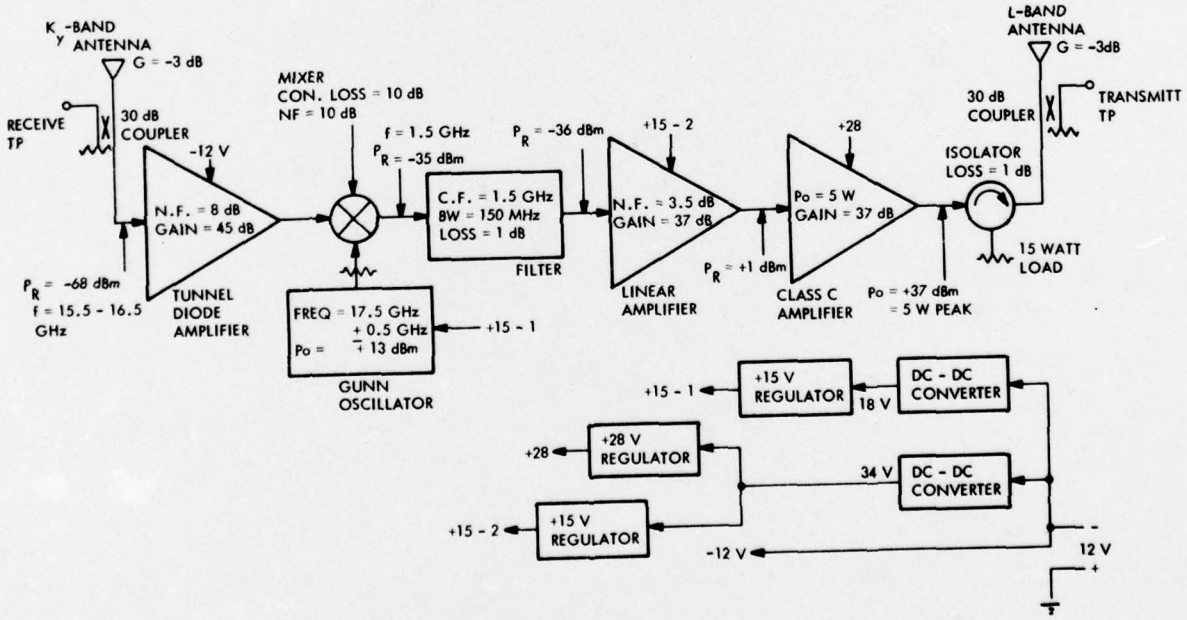

Figure 3-8. RTT Breadboard Heterodyne Repeater Configuration

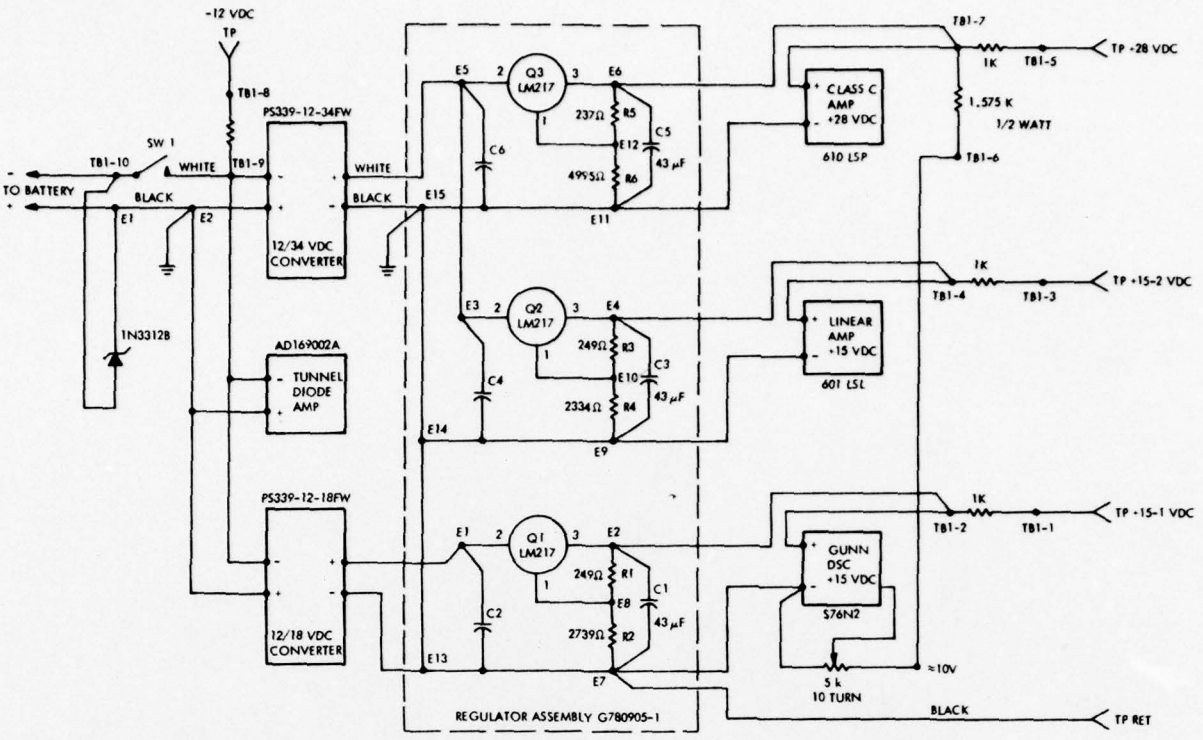

Figure 3-9. RTT-1 Repeater Power Supply Wiring Diagram

radiation during remote deployment. In order to improve radiation of the internally generated heat, the main chassis is anodized to provide a relatively high emissivity coefficient.

Table 3-1 summarizes the operating parameters and equipment specifications for the repeater unit.

Repeater Test Conditions and Results - The following paragraphs describe the test conditions and results of the heterodyne receiver unit.

Angle Coverage - The assembled repeater transmit and receive antenna patterns were measured in an anechoic chamber and the results are shown in Figures 3-10 and 3-11. Nominal gains are 0.2 dB for the Ku-Band and 2.5 dB (vertical polarization) for the L-Band.

Frequency Coverage - The LO is tunable to accommodate input signal frequencies 16 $\pm$ 0.5 GHz. The transmit frequency range is limited by the bandpass filter to 1500 $\pm$ 75 MHz.

Table 3-1. Repeater Unit Specifications

Ku-Band Antenna (W J 8569-1)		L-Band Antenna (Transco X11028500)	
Frequency Range	12 to 18 GHz	Frequency	500 - 2000 MHz
Polarization	Circular	Polarization	Vertical
Gain	+3 dBi (circularly polarized)	Gain	*3.5 dBi (Minimum)
Bandwidth		VSWR	2.5 (Maximum)
Azimuth	360°	Efficiency	85%
Elevation	20°	Pattern	* 1/4 λ Monopulse
Axial Ratio	2 dB Typical	Power	25 Watts (CW Maximum)
	5 dB Maximum		
Deviation From OMNI	+2 dB	*5 λ ground plane.	
VSWR	2.5		
Weight	16 oz		

Table 3-1. (Continued)

Ku-Band Preamplifier (AERCOM AD169002)	
Frequency	15 to 16.5 GHz
Noise Figure	8.5 dB (Maximum)
Gain	50 dB (Nominal)
Saturated Output Power	+10 dBm (Minimum)
Supply Voltage	-12 Vdc ± 10%
Supply Current	0.65 A (Nominal)

Local Oscillator (Wavetek S76N2)

Tuning Frequency Range	
Mechanical	17 to 18 GHz
Electrical (Varactor)	150 MHz
Power Out	30 mW Min
Supply Voltage	+15 Volts
Supply Current	0.5 Amp

Mixer (RHG dmH2-18)	
Frequency	
rf	2 to 18 GHz
if	1 to 8 GHz
Noise Figure	9 dB typical
Local Oscillator	11 dB Maximum
Lo Level	+10 dBm

Linear Amplifier (Amplica 601 LSL)

Frequency Range	1 to 2 GHz
Gain	37 dB (Minimum)
Noise Figure	3.5 dB (Maximum)
P_O (1 dB Comp)	+13 dBm
Gain Flatness	±1 dB
Intercept Point	+24 dBm (Typical)
VSWR - In	2
- Out	2
Supply Voltage	+15 V
Supply Current	80 mA

Table 3-1. (Continued)

Class C Amplifier (AMPLICA 610 LSP)	
Frequency Range	1.4 to 1.7 GHz
PO	5 watts (Minimum)
Gain	37 dB (Minimum)
Gain Flatness	±0.5 dB
VSWR - Input	1.5 (Maximum)
Rise Time (10-90 percent)	25 nsec (Maximum)
Pulse Position Uncertainty	4 ns
Dynamic Range	10 dB
Supply Voltage	+28 Vdc
Supply Current	0.25 A (No Output)
	1.0 A (5W CW)

Bandpass Filter (K&L 4B250-1500/150-0/R)	
Center Frequency	1500 MHz
3 dB Bandwidth	150 MHz
Number of Poles	4

DC - TO - DC Converters	
PS 339-12-34-FW	
Input	
Voltage	12 Vdc (Nominal)
Current	4 A (Maximum)
Output	
Voltage	34 Vdc (Nominal)
Current	1 A (Maximum)
Efficiency	75 Percent
PS 339-12-18-FW	
Input	
Voltage	12 Vdc (Nominal)
Current	4 A (Maximum)
Output	
Voltage	18 Vdc (Nominal)
Current	2 A (Maximum)
Efficiency	75 Percent

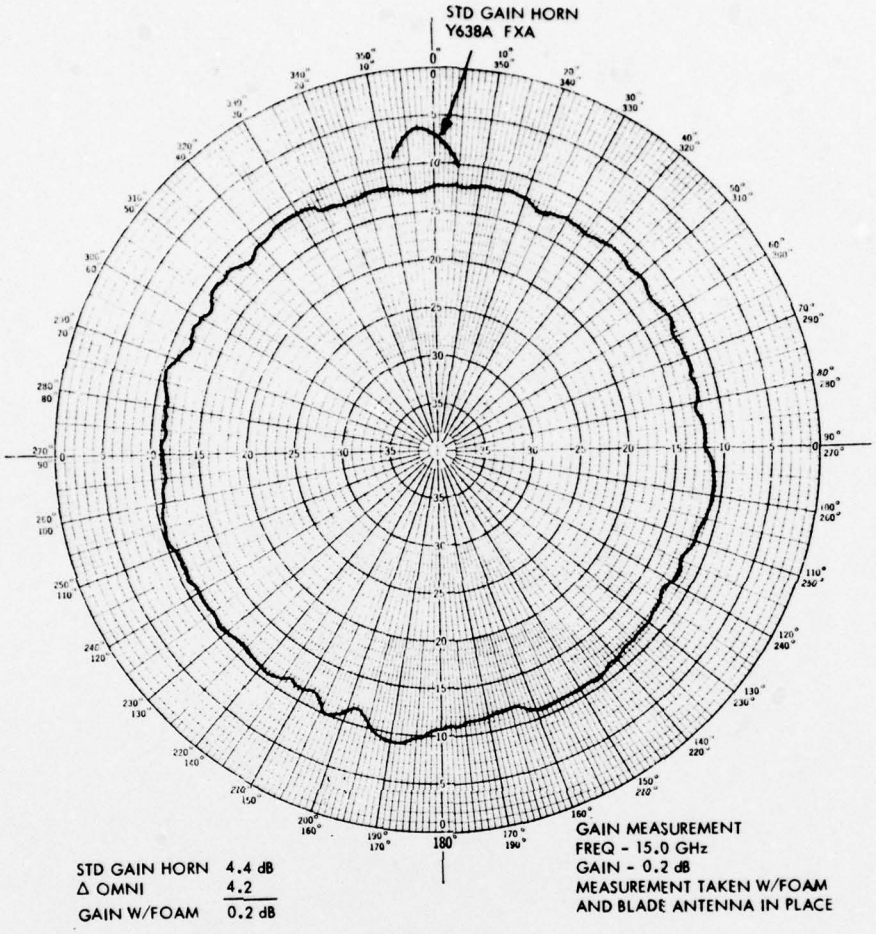

Figure 3-10. Measured Pattern for Ku-Band and L-Band Combined, Showing Uniformity of Gain vs. Angle

Frequency Drift - Measurements of output frequency shift due to the LO drift indicated a total shift of less than 6 MHz over an ambient temperature range 0-120^{o}F. The measured shift was less than 2 MHz per hour at room temperature.

Sensitivity - As deployed during the RTT-1 field tests, the measured signal required for saturated output was -65 dBm. The output power is approximately proportional to the input power for input signal levels less than 5 dB below saturation. No output is present for input signal levels below the -70 dB level.

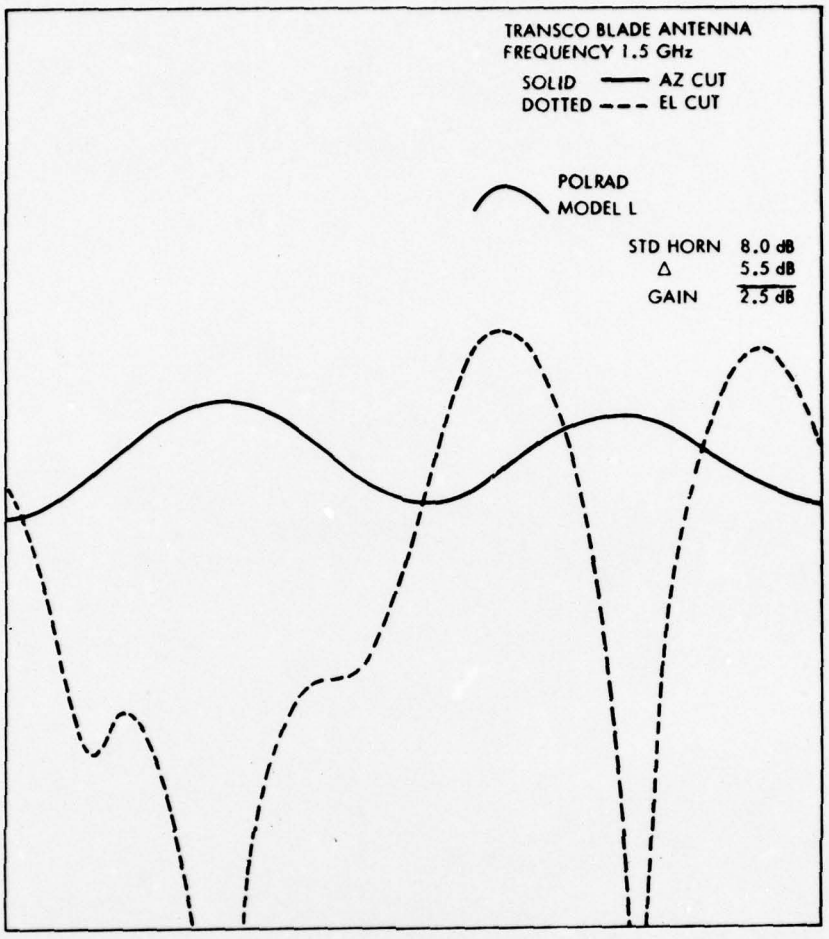

Figure 3-11. Pattern for Final Mounted L-Band Antenna Configuration

L-Band Output - The saturated output power for the repeater was measured at +40.7 dBm or 11.7 watts. Assuming an antenna gain of 2.5 dB (see Figure 3-11) the ERP was +43.2 dBm.

Time Delay - Figures 3-12, 3-13 and 3-14 show photographs of the detected input and output RF pulses for three input signal levels. This data provides an indication of the bias and variation introduced by the repeater during DTOA measurements. However, hard limiting in the base station receiver IF amplifiers precludes using a fixed level (such as 50% amplitude) as a basis for establishing the exact delay. Using the data shown, the delay for a -65 dBm signal is approximately 50 nanoseconds, decreasing to approximately 25 nanoseconds for a signal 30 dB above that level.

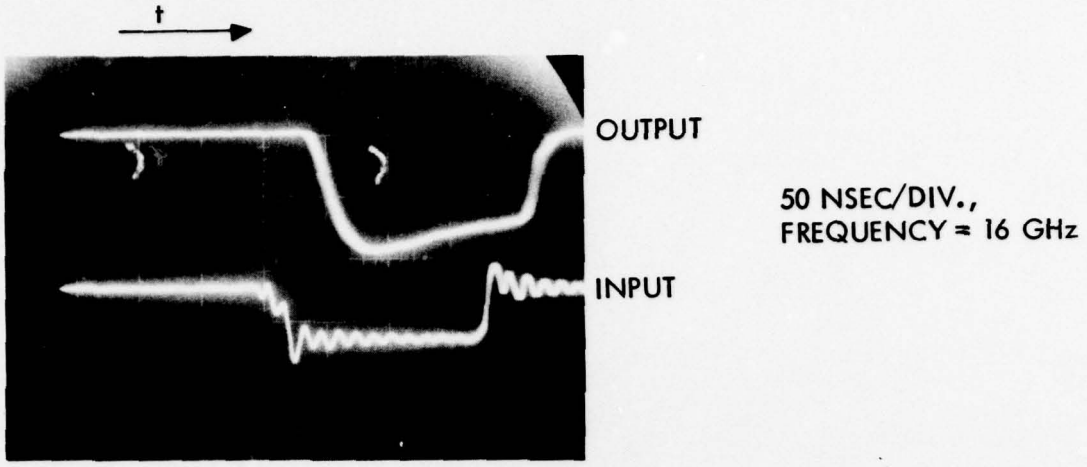

Figure 3-12. Detected RF Input and Output Pulses, Input Level = -65 dBm

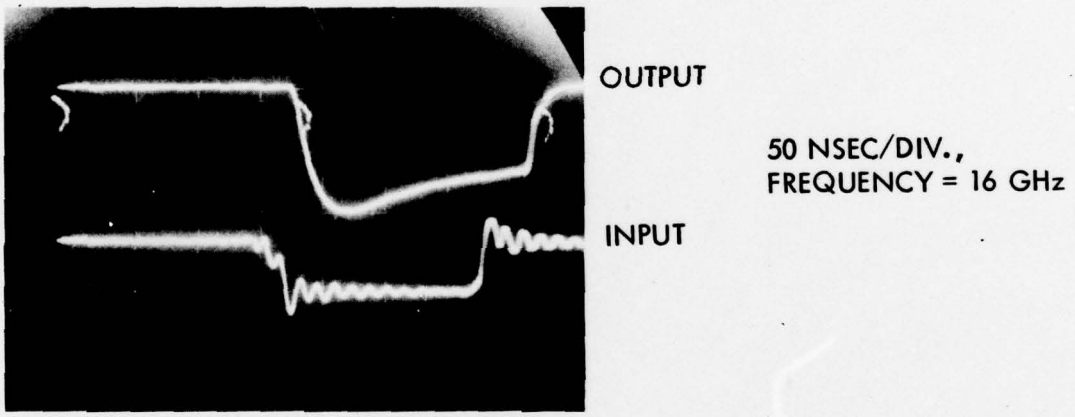

Figure 3-13. Detected RF Input and Output Pulses, Input Level = -49 dBm

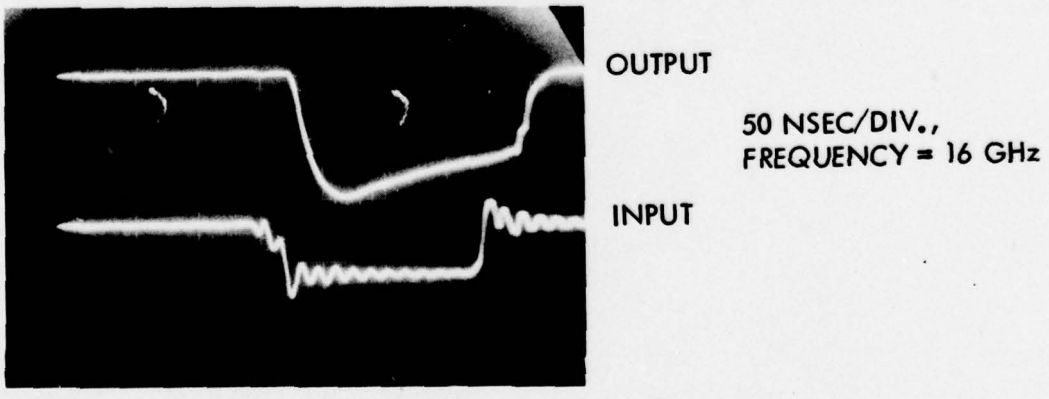

Figure 3-14. Detected RF Input and Output Pulses, Input Level = -35 dBm

Prime Power - Prime Power for the repeater is nominally -12 Vdc at 4.88 Amp for output duty cycles < 10%. A slight increase in prime power occurs up to 50% duty cycle at which time the output power decreases approximately proportional to the duty cycle. Normal operation includes an input voltage range of 11 - 12.5V.

3.2.2.4 Base Station - The base station consists of the antenna pedestal assembly, equipment rack assembly, and interrogate radar as shown in the photograph of Figure 3-15. A description of the interrogate radar is found in Section 3.2.2.2, and the two remaining assemblies are described in the subsequent paragraphs.

Antenna Pedestal Assembly - The antenna pedestal assembly consists of the L-Band antenna Ku-Band preamp and two azimuth positioners, as shown in Figure 3-15. Although not included in that figure, a theodolite mounting position is situated between the two antenna reflectors for aid in boresighting and as an optical check during DF measurements. A provision for local position control was included on the pedestal assembly to facilitate optical sighting. Specification/measured data are detailed in Table 3-2. for the various units.

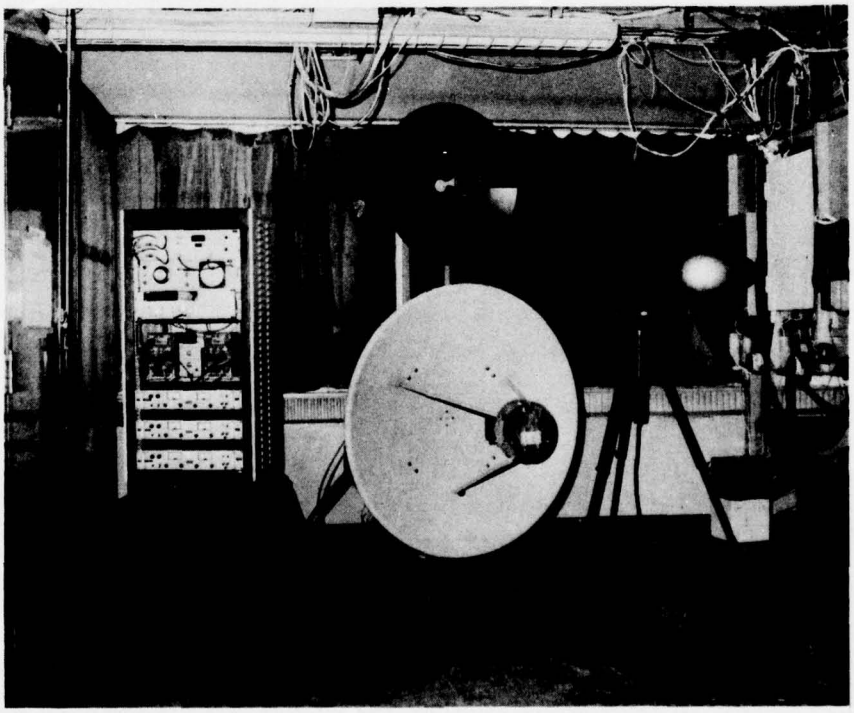

Figure 3-15. RTT-1 Base Station

Table 3-2. Antenna Pedestal Assembly, Measured Data

Azimuth Positioners (SA 5103-1/51030)	
Characteristics	
Total Bending Moment	200 ft-lbs
Total Vertical Load	200 lbs
Drive Motor Horsepower	1/15
Delivered Torque	102 ft-lbs
Withstand Torque	200 ft-lbs
Max. Full Load Operating Speed	1.1 rpm
Position Accuracy	0.05 degrees
Total Max. Drive Gear Backlash,	0.02 degrees
*Total Limit-to-Limit Travel (with option)	400 degrees
Turntable Diameter	12 inches
Center Access Hole Diameter	1-1/8 inches
Base Outside Diameter	(2) inches
Total Height	10 inches
Recommended Positioner Control	4111
Net Weight	60 lbs
*Limits Set at ±45 Degrees on Both Positioners	
Ku-Band Preamplifier (Aercom AD169002)	
Frequency, GHz	15.5 - 16.5
Noise Figure, dB	8.5 (maximum)
Gain, dB	50 (nominal)
Saturated Output Power dBm	+10 (minimum)
Supply Voltage Vdc	-12 +10%
Supply Current A	0.65 (nominal)
L-Band Preamplifier (Amplica 414LSL)	
Frequency, MHz	1050-1550
Noise Figure, dB	2.5 (maximum)
Gain, dB	38 (minimum)
Power Out at 1 dB Comp dBm	+10 (minimum)
Supply Voltage Vdc	+15
Supply Current mA	40 (nominal)

Ku-Band Antenna - The measured pattern and gain for the Ku-Band base station antenna is shown in Figure 3-16. As indicated, the sum channel gain was approximately 30.4 with a beamwidth of 2.1 degrees. Null depth in the difference pattern was 27 - 28 dB.

L-Band Antenna - The measured pattern and gain for the L-Band base station antenna is shown in Figure 3-17. As indicated, the sum channel gain is approximately 23.5 dB with a beamwidth of 15 degrees. Null depth in the difference pattern exceeds 30 dB.

Equipment Rack Assembly - The equipment rack assembly consists of the RF tuners, positioner, control, time delay processor, counter and power supplies.

Specifications are listed in Table 3-3 for the positioner control, RF tuners and major subassemblies of the time delay processor. The time delay processor and counter are discussed in separate paragraphs.

Time Delay Processor and Counter - Figure 3-18 shows a block diagram of the time delay processing including the counter interface. As originally configured, an operator-selected number of start-stop pulse intervals was to be averaged with a "bad data" indication appearing in the event that the number of "start" and "stop" pulses was unequal. It was later determined that this approach conflicted with the time interval averaging operational mode of the HP 5345A counter, which accumulates total time. Consequently, the system was operated with the time delay processor set for 255 intervals and the actual number of intervals determined by the counter. The display on the panel was used to indicate the actual number of intervals averaged by the counter while the counter display indicated the average time interval between "start" and "stop" pulses. Due to the fact that the counter gate time selections are in decade increments, the number of intervals averaged was a function of the interval magnitude. The minimum number was 25 and the maximum was 255 for contiguous intervals. The following is a listing of the switch selection required on HP 5345A counter.

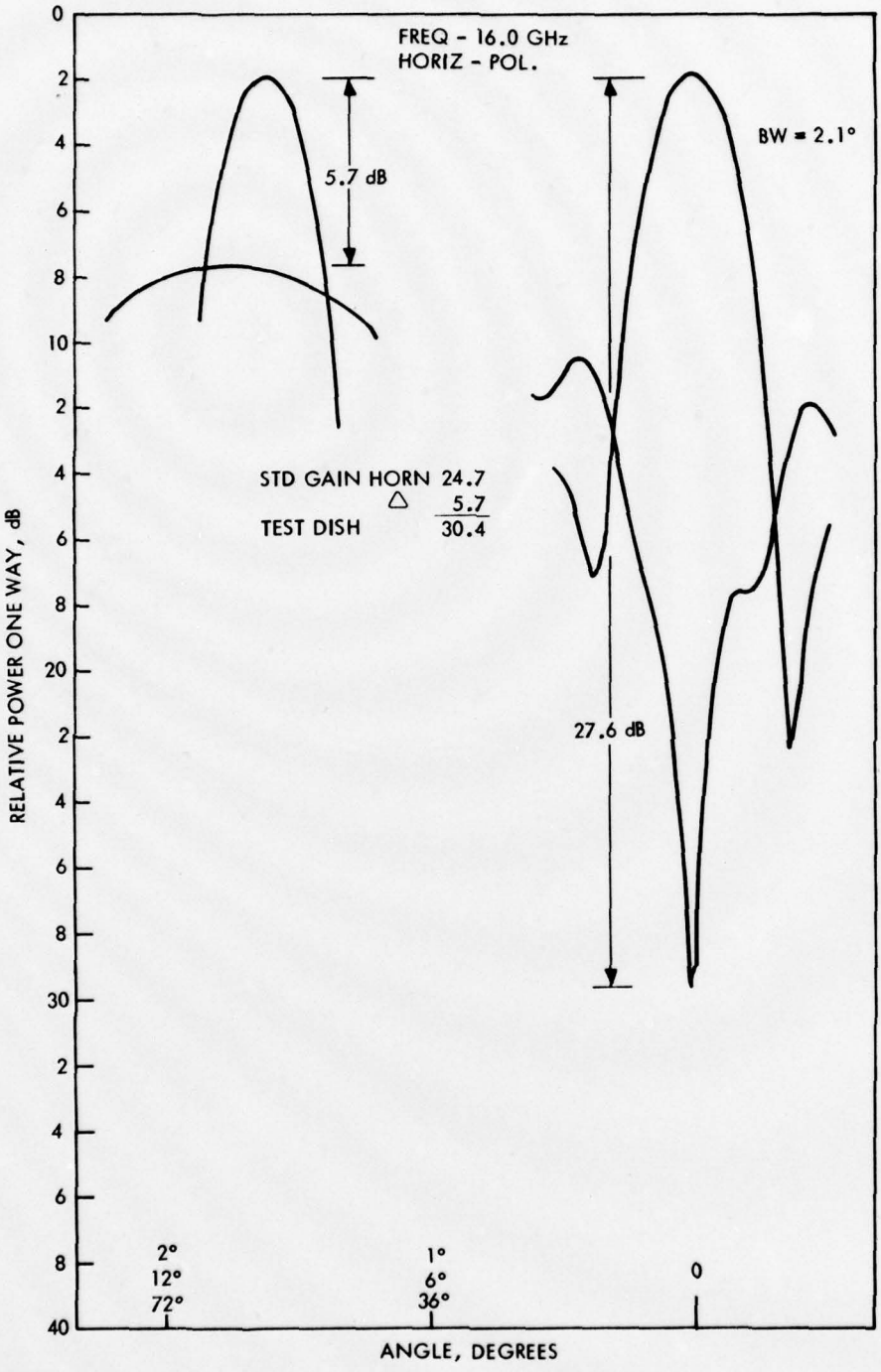

Figure 3-16. Base Station Ku-Band Sum and Difference Antenna Pattern, Showing Null Depth

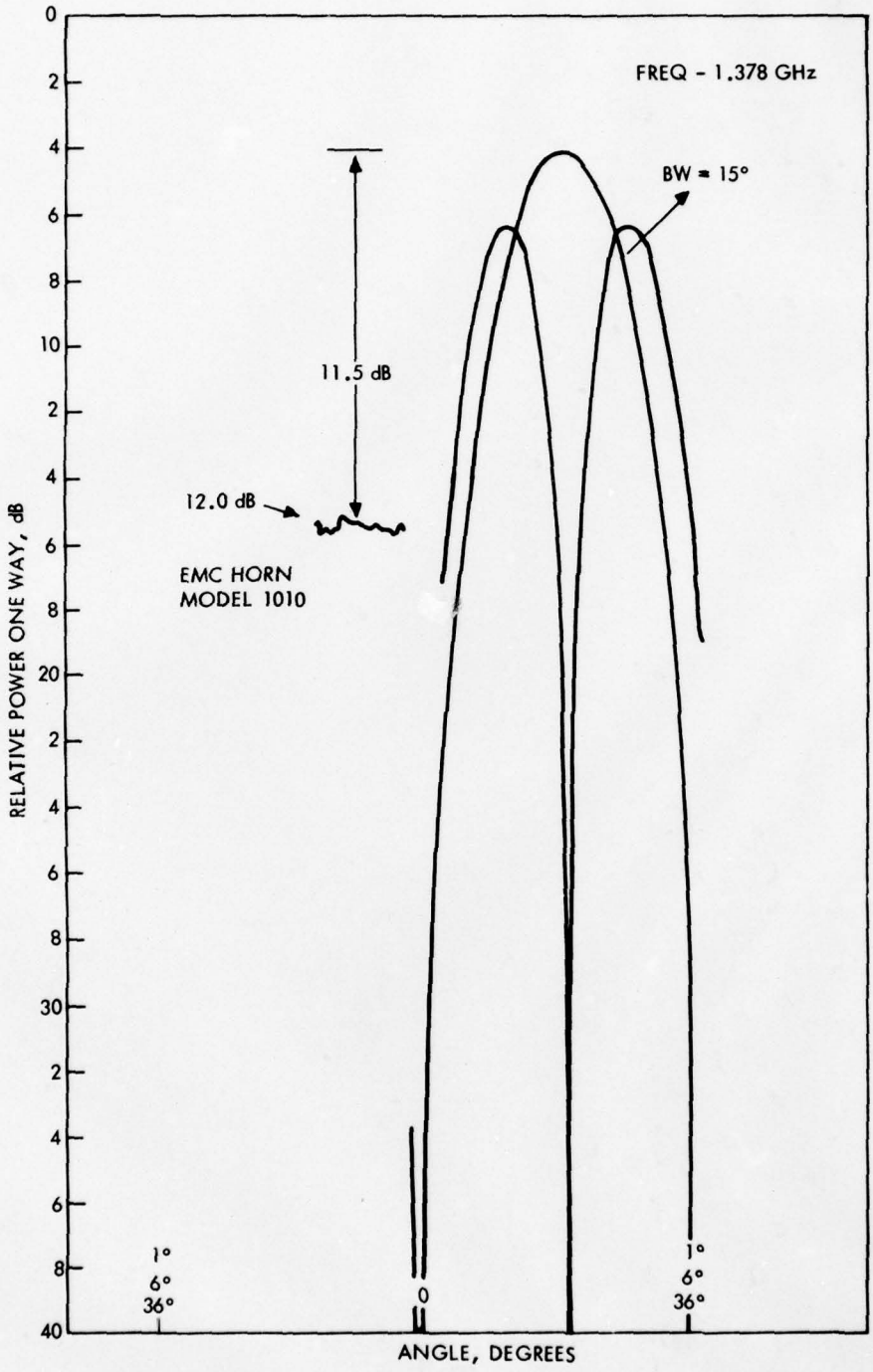

Figure 3-17. Base Station L-Band Sum and Difference Antenna Pattern, Showing Null Depth

Table 3-3. Positioner Control Specifications

SCI Tuners

Frequency Range	RT102C	RT1218C
Noise Figure, Typical, Without Preamplifier	13	16
Noise Figure, Maximum, Without Preamplifier (dB)	14	18
Frequency Resettability, Typical (±%)	0.02	0.05
Incidental FM, Typical, RMS	1	3
Incidental FM, Maximum, RMS	3	8
Incidental FM, Typical, Peak-to-Peak (kHz)	5	12
Incidental FM, Maximum, Peak-to-Peak (kHz)	10	30

Limiting IF Amplifiers (Rhg ICSL 16020)

Center Frequency	160 MHz
Bandwidth	20 MHz
Power Output	+10 dBm (nominal)
Input Dynamic Range	-70 to -5 dBm
Phase Shift over Input Range	10 Degrees
Output Variation over Input Range	0.5 dB
Noise Figure	10 dB
Input Impedance	50 ohms
Input VSWR	1.5:1 max
Output Impedance	50 ohms
Output VSWR	1.5:1 max

Table 3-3. (Continued)

Detectors (Alan 50D-2)	
Frequency Range	100 kHz to 0.5 GHz
Frequency Response	± 1.5 dB
Input Impedance	50 ohms
Output Polarity	positive
VSWR Maximum	1.2:1 at maximum frequency
Tangential Signal Sensitivity	-40 dBm min
Connectors, RF IN	BNC
Connectors, DC OUT	BNC
Maximum Input Power	1 Watt
Positioner Control (SA 4111-1)	
Includes Dual Speed Indicator	1:1 and 36:1

Input Switch Settings (Front Panel)

Function	-	Time Int A to B
Gate Time	-	(Function of Delay)
Level	-	Preset
Impedance	-	50 ohms
Attenuation	-	X1
Coupling	-	DC
Slope	-	Positive
Mode	-	Separate

Rear Panel

Gate Control Input	-	Ext Arm

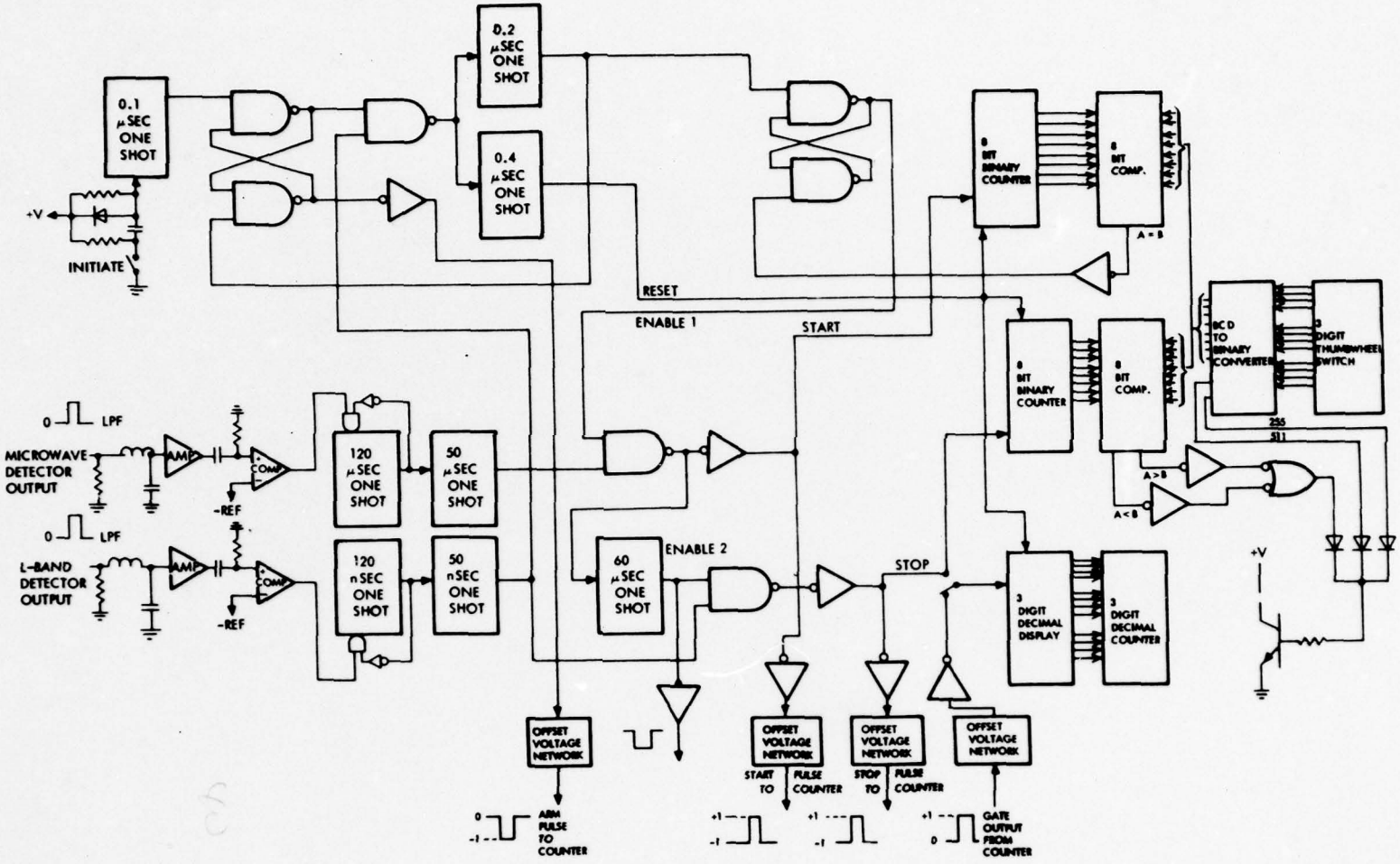

Figure 3-18. Time Delay Processor and Counter Block Diagram

In order to eliminate possible multipath responses, both "start" and "stop" channels were disabled by a latch for approximately one-half of the victim/interrogate pulse repetition period (i.e., 120 microseconds). The comparator's reference levels were set to approximately 0.6 of the limited signal level after detection. The LPF consisted of a single LC section with a cutoff frequency of 10 MHz. The amplifiers following the LPF sections were video amplifiers with a bandwidth of 40 MHz.

3.3 TEST PLAN

Field testing was divided into three areas:

1. Multipath propagation effects testing
2. Foliage obstruction effects testing
3. Terrain obstruction effects testing

Of these, the first was the most comprehensively treated. Quantitative data regarding ground-to-ground multipath is meager, yet this appears to be the most uncertain aspect of the RTT-1 concept technical feasibility. Accordingly, this area received primary attention.

Foliage and terrain obstruction effects, conversely, have been thoroughly examined by other investigators. Techniques permitting projection of their impact on system performance are available. Effort here was directed toward ascertaining that the expected mechanisms did indeed assert themselves and to determine whether other, unsuspected, phenomena might also be involved.

3.3.1 Test Scenario

Field testing was conducted at the Wayside Test Area, U.S. Naval Ammunition Depot, Earle, New Jersey, during June 1979.

The testing geometry used for multipath propagation effects test is shown in Figure 3-19. The equipment locations were situated in a large, relatively flat, open area surrounded by trees of 20 to 40 feet height. The terrain here consisted

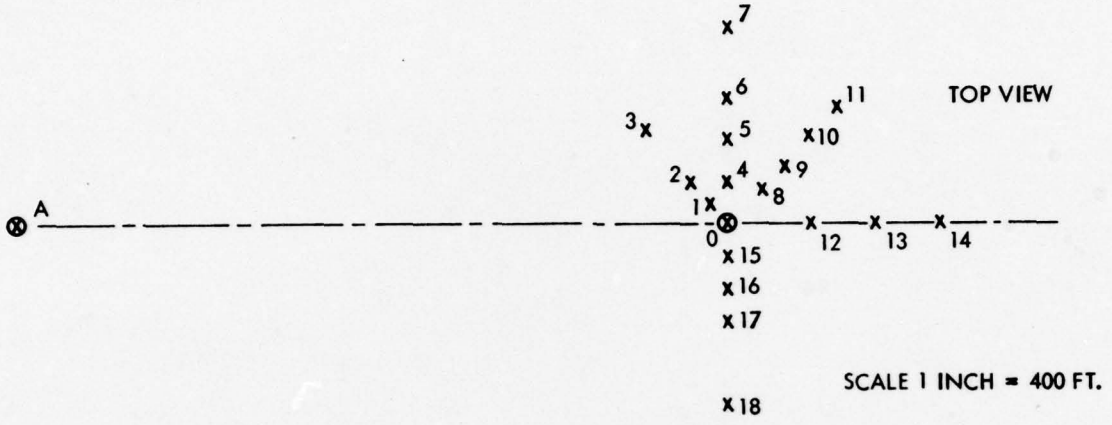

Figure 3-19. Multipath Propagation Effects Test Geometry

of patches of open gravel and grass one to two feet high. A gravel road ran its length, but this was not used during testing. Nor were vehicles parked where their reflections would impact tests.

The geometry used for foliage/terrain obstruction effects examination is shown in Figure 3-20. In addition to the elevation irregularity shown in the figure, the entire range was bounded by trees of 20 to 40 feet height. Those pertinent to foliage attenuation measurements are indicated in the figure.

All designated equipment sites were located by survey prior to the initiation of testing. Relative site locations were accurate to within ± 2 feet.

Although it rained prior to and during the two-week testing interval, all test operations were conducted during clear, usually sunny weather.

3.3.2 Test Procedures

Based upon data collection needs and test system operational experience acquired, prior to field testing, at RCA Burlington, Massachusetts, procedures were established for field calibration of the test system, and for accomplishing the field tests themselves. They are presented in Tables 3-4 and 3-5, respectively.

In practice, the system was calibrated at least once each day. The results of calibration were used to assure proper system operation and to acquire DTOA bias estimates for use in conducting on-site error analysis.

Table 3-4. Field Calibration Procedures

1. Locate base station at designated location and level using jacks.
2. Rotate <u>top</u> positioner until L and Ku band antennas are approximately boresighted together.
3. Connect base station for repeater interrogation (see Figure 3-21) and deploy repeater at surveyed location in-line with victim radar location.
4. Install appropriate attenuators in system and record on data sheet.
5. With positioner control and read-out connected to bottom positioner, locate L-band null position using L-band limiting IF amplifier output. Retune SCI receiver as necessary. Record null position $\left[\theta_{R(RF\text{-}CAL)}\right]$ on data sheet.
6. Connect positioner control and read-out to top positioner and confirm that Ku band interrogate antenna is approximately centered on repeater.
7. Carefully tune both SCI receivers so that signals are centered in bandwidth.
8. Perform time difference measurement several times with counter setting adjusted so that at least 20 periods are averaged during each measurement. Record measured data $\left[\Delta\tau_2\right]$ in data sheet.
9. Install appropriate attenuators in system and record on data sheet.
10. Remove PPS-5 transmitter from base station and assemble PPS-5 radar at surveyed victim radar location. Connect base station system for DTOA measurements. See Figure 3-22.
11. Using PPS-5 radiated signal, null Ku band output at base station with top positioner. Record null position $\theta_{V(RF\text{-}CAL)}$ on data sheet.
12. Rotate theodolite by hand until centered on victim radar and lock in position.
13. Repeat Step 7. Record measured data $\left[\Delta\tau_D\right]$ on data sheet.
14. Based upon comparison of the results of Step 7 measurements with surveyed base station to repeater range, compute $\tau_2(Bias)$.
15. Based upon comparison of the results of Step 11 measurements with surveyed difference in path ranges, compute $\tau_D(Bias)$.

Table 3-5. Field Test Procedures

1. Connect base station system for repeater interrogation (see Figure 3-21) and deploy repeater at surveyed location.
2. Install appropriate attenuators in system and record on data sheets.
3. With positioner control and read-out connected to bottom positioner, locate L-band null position using L-band limiting IF amplifier output. Retune SCI receiver as necessary. Record null position $\left[\theta_R(RF)\right]$ on data sheet.
4. Connect positioner control and read-out to top positioner and co-align Ku band interrogate antenna with L-band antenna.
5. Carefully tune both SCI receivers so that signal is centered in bandwidth.
6. Perform time difference measurement several times with counter setting adjusted so that at least 20 pulse interval periods are averaged. Record measured data ($\Delta\tau_2$) in data sheet.
7. Remove PPS-5 transmitter from base station and assemble PPS-5 radar at surveyed victim radar location.
8. Install appropriate attenuators in system and record on data sheet.
9. Using PPS-5 radiated signal, null Ku band output at base station with top positioner. Record null position $\left[\theta_V(RF)\right]$ on data sheet.
10. Rotate theodolite using positioner control until centered on repeater. Record positioner read-out $\left[\theta_V(OPT)\right]$.
11. Repeat Step 6 procedure. Record measured data ($\Delta\tau_D$) on data sheet.
12. Compare $\theta_V(OPT)$ with $\theta_V(RF)$ to determine error.
13. Subtract $\Delta\tau_2(BIAS)$ from $\Delta\tau_2$ to obtain $\Delta\tau_2'$.
14. Subtract $\Delta\tau_D(BIAS)$ from $\Delta\tau_D$ to obtain $\Delta\tau_D'$.
15. Subtract $\theta_V(RF\text{-}CAL)$ from $\theta_V(RF)$ to obtain $\eta(RF)$.
16. Using $\eta(RF)$, $\Delta\tau_2'$, and $\Delta\tau_D'$, compute victim radar range.
17. Compare the results of Step 14 with surveyed victim radar range.

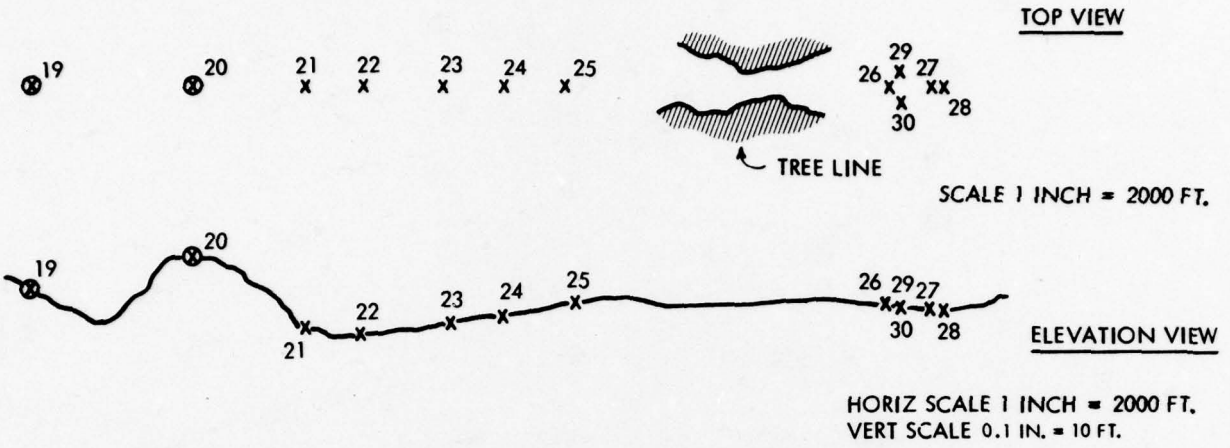

Figure 3-20. Foliage/Terrain Obstruction Effects Test Geometry

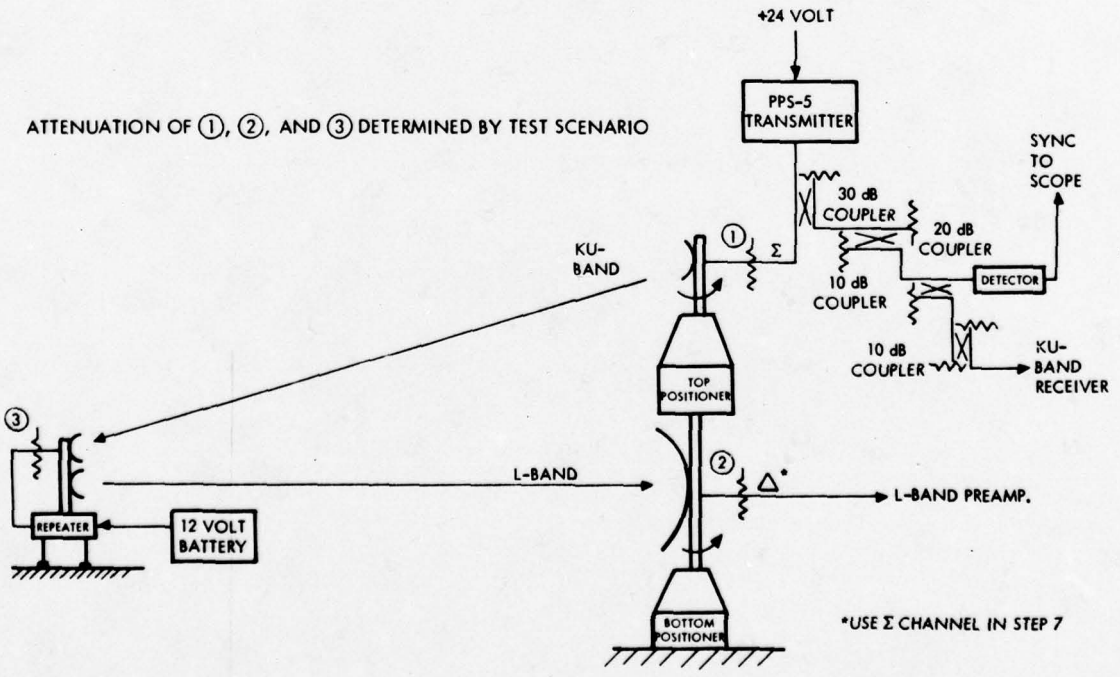

Figure 3-21. System Connection for Repeater Interrogation

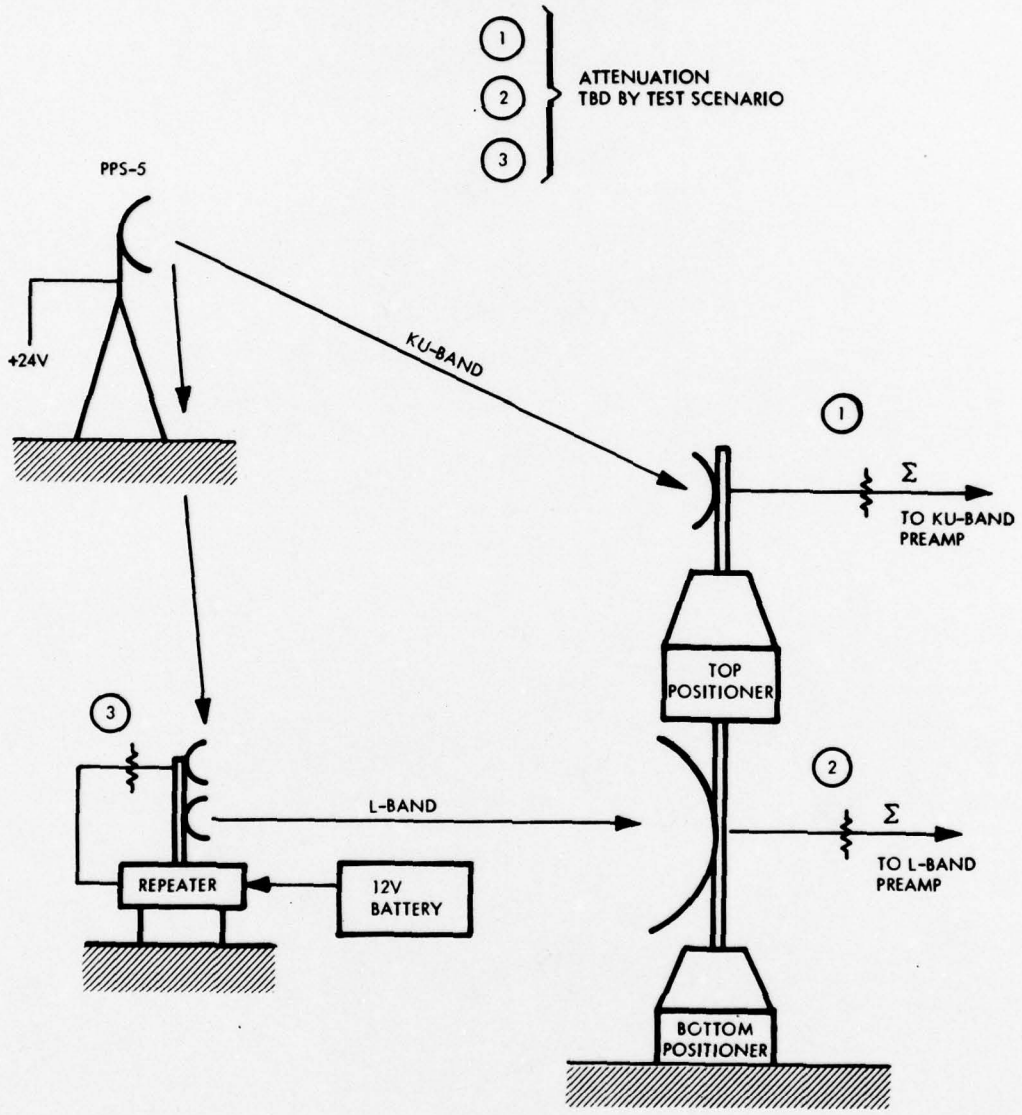

Figure 3-22. System Connection for DTOA Measurement

SECTION 4

SECTION 4
RESULTS

4.1 MULTIPATH EFFECTS EXAMINATION RESULTS

4.1.1 Data Reduction Process

The raw data contained on the field test data sheets consisted of measured values for $\Delta\tau_2$, $\Delta\tau_D$, θ_V(RF), θ_V(OPT) and η. This was processed as indicated in Figure 4-1. Only primary data was used. The results of on-site error analysis used to monitor daily results were disregarded during the post-test analysis.

The raw measurement data and survey information were compared and analyzed to identify the mean and standard deviation associated with each measurement process error. The mean error values were considered measurement system biases - legitimately extractable from raw measurements in assessing system performance. The error standard deviations were used both as a basis to upgrade the system analytical model and as a cross-check on field test performance versus analytical projections.

RTT-1 performance analysis consisted of recomputing the victim radar location, using the raw measurement data with the biases extracted. The resultant location was compared with the actual, surveyed, location to determine location error. This error was then compared to the analytically forecasted system location error as a cross-check on the results.

The RTT-1 analytical model was upgraded by modifying the measurement error standard deviation distribution to more accurately reflect the error contributions encountered in the field, i.e., the impact of multipath effects on system operation.

Using the upgraded analytical model, the reduced-range field test results were extrapolated to reflect the performance expected at near maximum operational range. The model was also used to examine the impact of varying levels of measurement accuracy upon overall system performance, thus assessing the effect of state-of-the-art technology on achievable system performance.

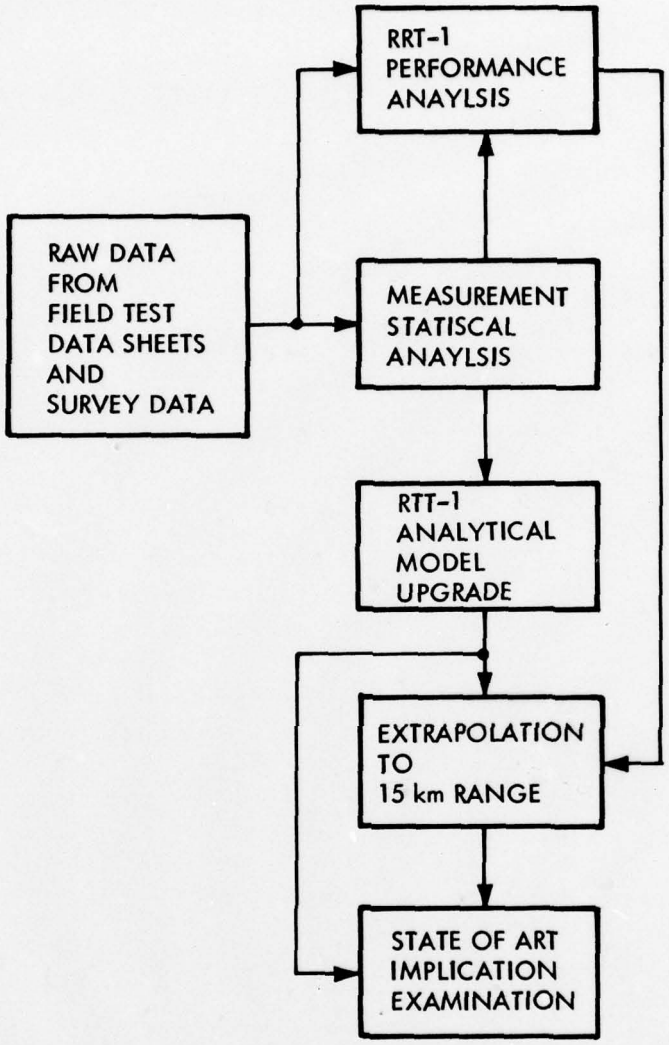

Figure 4-1. Multipath Effects Examination Data Reduction Process

4.1.2 Statistical Analysis of Measurement Data

The results of measurements made during field tests were analyzed to identify the mean and standard deviation of the measurement process errors. This was required for two reasons:

1. The RTT-1 test system was recently assembled and very little data existed describing its performance regarding bias errors. In effect, a data base was established during testing.
2. It was expected (and subsequently confirmed) that multipath-induced errors would dominate system performance characteristics. These errors most directly manifest themselves in the measurement processes and are most readily quantified there.

Table 4-1 lists surveyed range and angle parameters for the test range geometry shown in the preceding section. These factors were used as the standards against which measurement results were compared. The Location Codes column identifies each combination of base station, victim radar and repeater examined. The Test Number column identifies the test (or tests) accomplished at that location.

Table 4-2 contains essential data relevant to the DF measurement error analysis. It is noted that RTT-1 test procedures did not accommodate direct readout of θ_R, the repeater location angle. This parameter was calculated from the measured data.

Table 4-3 contains the data associated with the TOA (for range to the repeater) and DTOA measurement error analysis.

It was noted, during testing, that in certain areas of the test range, multipath effects intensified. One test (number 11) was repeated (number 25) to examine repeatability under these conditions. All data collected has been used in establishing the statistical data base. Although the error behavior is generally gaussian, it should be recognized that behavior in individual regions can vary in a decidedly non-gaussian manner.

4.1.3 RTT-1 Performance Analysis

The objective of this data reduction task was to examine the performance of the RTT-1 test system in the field regarding its conformity to analytical projections. This was an essential step in assuring that extrapolation of the results to more operationally significant situations be accurate.

Table 4-1. Surveyed Range/Angle Parameters

Location Code	Test No.	Function	R_1 (ft)	R_2 (ft)	R_d (ft)	ΔR (ft)	η (deg)
A-0-1	5	Meas	70	1574.2	1623	21.2	1.80
A-0-2	6	Meas	150	1520.5	1623	47.5	4.00
A-0-3	7	Meas	260	1450.8	1623	87.8	7.27
A-0-4	9	Meas	90	1625.4	1623	94.2	3.17
A-0-5	10	Meas	190	1634.0	1623	201.0	6.68
A-0-6	11	Meas	290	1648.5	1623	315.5	10.13
A-0-6	25	Meas(Rpt)	290	1648.5	1623	315.5	10.13
A-0-7	12	Meas	430	1678.7	1623	485.7	14.84
A-0-8	14	Meas	85	1684.1	1623	146.1	2.05
A-0-9	15	Meas	165	1743.5	1623	285.5	3.84
A-0-10	16	Meas	255	1812.2	1623	444.2	5.71
A-0-11	17	Meas	377	1898.3	1623	652.3	8.08
A-0-12	1	Calib	180	1803.0	1623	360.0	0.003
A-0-12	2	Calib	180	1803.0	1623	360.0	0.003
A-0-12	8	Calib	180	1803.0	1623	360.0	0.003
A-0-12	13	Calib	180	1803.0	1623	360.0	0.003
A-0-12	18	Calib	180	1803.0	1623	360.0	0.003
A-0-12	24	Calib	180	1803.0	1623	360.0	0.003
A-0-13	3	Meas	330	1953.0	1623	660.0	0.006
A-0-14	4	Meas	470	2093.0	1623	940.0	0.008
A-0-15	19	Meas	75	1624.8	1623	76.8	2.65
A-0-16	20	Meas	150	1630.0	1623	157.0	5.28
A-0-17	21	Meas	220	1638.0	1623	235.0	7.72
A-0-18	18	Meas	419	1676.5	1623	472.5	14.47

Table 4-2. DF Measurement Error Analysis

Location Code	Test No.	Function	(1) θ_V(Opt) (deg)	(2) θ_V(DF) (deg)	(3) $\epsilon(\theta_V)$ (deg)	(4) η(Calc) (deg)	(5) η(DF) (deg)	(6) $\epsilon\eta$ (deg)	(7) $\epsilon\theta_R$ (deg)
A-0-1	5	Meas	+3.08	+3.25	+0.17	-1.80	-2.05	-0.25	-0.08
A-0-2	6	Meas	+4.60	+4.90	+0.30	-4.00	-3.70	+0.30	+0.60
A-0-3	7	Meas	+8.04	+8.20	+0.16	-7.27	-7.00	+0.27	+0.43
A-0-4	9	Meas	+4.25	+4.25	0.00	-3.17	-3.20	-0.03	-0.03
A-0-5	10	Meas	+7.32	+7.32	0.00	-6.68	-6.27	+0.38	+0.38
A-0-6	11	Meas	+10.20	+10.20	0.00	-10.13	-8.97	+1.16	+1.16
A-0-6	25	Meas Rep	+10.05	+10.05	0.00	-10.13	-9.85	+0.28	+0.28
A-0-7	12	Meas	+15.55	+15.70	+0.15	-14.84	-14.70	+0.14	+0.29
A-0-8	14	Meas	+1.85	+1.85	0.00	-2.05	-1.65	+0.40	+0.40
A-0-9	15	Meas	+3.88	+3.88	0.00	-3.84	-3.68	+0.16	+0.16
A-0-10	16	Meas	+5.95	+5.95	0.00	-5.71	-5.75	-0.04	-0.04
A-0-11	17	Meas	+7.95	+7.95	0.00	-8.08	-7.75	+0.33	+0.33
A-0-12	1	Calib	-	-	-	0.00	-	-	-
A-0-12	2	Calib	-	-	-	0.00	-	-	-
A-0-12	8	Calib	-	-	-	0.00	-	-	-
A-0-12	13	Calib	-	-	-	0.00	-	-	-
A-0-12	18	Calib	-	-	-	0.00	-	-	-
A-0-12	24	Calib	-	-	-	0.00	-	-	-
A-0-13	3	Meas	+1.20	+1.20	0.00	+0.01	0.00	-0.01	-0.01
A-0-14	4	Meas	+0.73	+0.73	0.00	+0.01	+0.47	+0.46	+0.47
A-0-15	19	Meas	-2.20	-2.20	0.00	+2.65	+2.80	+0.15	+0.15
A-0-16	20	Meas	-5.05	-5.05	0.00	+5.28	+5.65	+0.28	+0.28
A-0-17	21	Meas	-7.80	-7.80	0.00	+7.72	+8.40	+0.68	+0.68
A-0-18	22	Meas	-14.60	-14.60	0.00	+14.47	+15.20	+0.73	+0.73
					$m = +0.043^\circ$			$m = +0.30^\circ$	$m = +0.34^\circ$
					$\sigma_{\theta_V} = 0.089^\circ$			$\sigma_\eta = 0.36^\circ$	$\sigma_{\theta_R} = 0.32^\circ$

1. Meas by Theodolite
2. Meas by Wave DF
3. θ_V(OPT) - θ_V(DF)
4. From Survey Data
5. σ_V(DF) - θ_V(DF-CALIB)
6. η(DF) - η(CALC)
7. $\epsilon(\tau_i) + \epsilon(\theta_V)$

Table 4-3. TOA/DTOA Measurement Error Analysis

Location Code	Test No.	Function	τ_2(Act) (nsec)	τ_2(Meas) (nsec)	$\epsilon(\tau_2)$ (nsec)	τ_D(Act) (nsec)	τ_D(Meas) (nsec)	$\epsilon(\tau_D)$ (nsec)	Comments from Data Sheets
A-0-1	5	Meas	3201.9	3293.2	91.3	21.6	99.1	67.5	
A-0-2	6	Meas	3092.7	3182.0	89.3	48.3	119.7	71.4	
A-0-3	7	Meas	2950.9	3074.6	123.7	89.3	166.9	77.6	
A-0-4	9	Meas	3306.1	3378.4	72.3	94.0	183.0	89.0	
A-0-5	10	Meas	3323.6	3433.1	109.5	204.4	328.6	124.2	Non LOS to Rep
A-0-6	11	Meas	3353.0	3457.6	104.6	320.9	500.1	179.2	Multipath noted
A-0-6	25	Meas Rep	3353.0	3473.0	120.0	320.9	437.0	116.1	Multipath Region
A-0-7	12	Meas	3414.5	3509.5	95.0	494.0	617.9	123.9	Multipath Region
A-0-8	14	Meas	3425.5	3572.5	147.0	148.6	187.5	38.9	
A-0-9	15	Meas	3546.3	3644.2	97.9	290.4	344.9	54.5	
A-0-10	16	Meas	3686.0	3810.7	124.7	451.8	513.2	61.4	
A-0-11	17	Meas	3861.1	3996.3	135.2	663.4	742.3	78.9	
A-0-12	1	Calib	3667.3	3777.9	110.6	366.1	452.2	86.1	
A-0-12	2	Calib	3667.3	3769.2	101.9	366.1	443.3	77.2	
A-0-12	8	Calib	3667.3	3794.9	127.6	366.1	442.1	76.0	
A-0-12	13	Calib	3667.3	3787.6	120.3	366.1	427.0	60.9	
A-0-12	18	Calib	3667.3	3771.3	104.0	366.1	430.4	64.3	
A-0-12	24	Calib	3667.3	3770.2	102.9	366.1	439.0	72.9	
A-0-13	3	Meas	3972.4	4077.6	105.2	671.2	749.2	78.0	
A-0-14	4	Meas	4257.2	4337.6	80.4	956.0	1023.5	67.5	
A-0-15	19	Meas	3304.8	3413.7	108.9	78.1	143.5	65.4	
A-0-16	20	Meas	3315.4	3398.3	82.9	159.7	233.6	73.9	
A-0-17	21	Meas	3331.7	3428.8	97.1	239.0	325.8	86.8	
A-0-18	22	Meas	3410.0	3496.3	86.3	480.5	595.1	114.6	
			nsec	nsec	nsec	nsec	nsec	nsec	

$\tau_2(\text{BIAS}) = 105.8$ nsec $\qquad \tau_D(\text{BIAS}) = 83.6$ nsec

$\frac{1}{C} = 1.017$ nsec/ft $\qquad \sigma_{TOA} = 18.2$ nsec $\qquad \sigma_{DTOA} = 29.6$ nsec

$\tau_D(\text{Act}) = \frac{\Delta R(\text{Surv})}{C} \qquad \tau_2(\text{Act}) = \frac{2R_2(\text{Surv})}{C}$

Table 4-4 summarizes the computations associated with extraction of system bias errors from the measurement results. Table 4-5 lists RTT-1 measured versus surveyed values of victim radar location in terms of range and angle. Range error and deflection error are also presented. Table 4-6 compares RTT-1 measured range error with analytically projected error.

In making the analytical projections, the random error components (σ_{TOA}, σ_{DTOA} and σ_η) identified in Tables 4-1 and 4-2 were used. In general, the RTT-1 test system performed in a statistically predictable manner.

4.1.4 Analytical Model Upgrade

Adjustment of the RTT-1 analytical model to reflect operation in the presence of multipath consisted of establishing error schedules which matched the test-derived values for σ_{TOA}, σ_{DTOA} and σ_η, accounting for all of their known or calculable subcomponent values and including subcomponents attributable to multipath in a consistent manner. In the case of $\sigma\eta$, this was accomplished in a straightforward manner. In the case of σ_{TOA} and σ_{DTOA}, this was not possible and some analytical judgement was, of necessity, supplied.

An essential input to this analysis is the S/N environment in each RTT-1 link during the tests. This data is presented in Table 4-7. Since the range of S/N values (calculated using surveyed ranges and known system parameters) is small, an average value for each link is identified and its impact on time and angle measurements calculated.

σ_η Considerations

The value identified for $\sigma\eta$ in Table 4-2 is 0.36°. This value should relate to error subcomponents in accordance with the following expression:

$$\sigma_\eta = \sqrt{\sigma^2_{SYS} + \sigma^2_{\theta\ V\text{-}N} + \sigma^2_{\theta\ V\text{-}M} + \sigma^2_{\theta\ R\text{-}N} + \sigma^2_{\theta\ R\text{-}M}} \qquad (4\text{-}1)$$

Table 4-4. Measurement Error Bias Extraction

Location Code	Test No.	Function	τ_2 (Meas)	τ_2 (Bias)	(1) τ_2'	τ_D (Meas)	τ_D (Bias)	(2) τ_D'	η(Meas)	η(Bias)	(3) η'
A-0-0	-	Not Used	-	-	-	-	-	-	-	-	-
A-0-1	5	Meas	3293.2	105.8	1593.7	99.1	83.6	15.5	-2.05°	0.3°	-2.35°
A-0-2	6	Meas	3182.0	105.8	1538.1	119.7	83.6	36.1	-3.70°	0.3°	-4.05°
A-0-3	7	Meas	3074.6	105.8	1484.4	166.9	83.6	83.3	-7.00°	0.3°	-7.30°
A-0-4	9	Meas	3378.4	105.8	1636.3	183.0	83.6	99.4	-3.20°	0.3°	-3.50°
A-0-5	10	Meas	3433.1	105.8	1663.7	328.6	83.6	245.0	-6.27°	0.3°	-6.57°
A-0-6	11	Meas	3457.6	105.8	1675.8	500.1	83.6	416.5	-8.97°	0.3°	-9.27°
A-0-6	25	Meas Rep	3473.0	105.8	1683.6	437.0	83.6	353.4	-9.85°	0.3°	-10.15°
A-0-7	12	Meas	3509.5	105.8	1701.9	617.9	83.6	534.3	-14.7°	0.3°	-15.0°
A-0-8	14	Meas	3572.5	105.8	1733.4	187.5	83.6	103.9	-1.65°	0.3°	-1.95°
A-0-9	15	Meas	3644.2	105.8	1769.2	344.9	83.6	261.3	-3.78°	0.3°	-4.08°
A-0-10	16	Meas	3810.7	105.8	1852.5	513.2	83.6	429.6	-5.78°	0.3°	-6.05°
A-0-11	17	Meas	3996.3	105.8	1945.3	742.3	83.6	658.7	-7.75°	0.3°	-8.05°
A-0-12	1	Calib	-	-	-	-	-	-	-	-	-
A-0-12	2	Calib	-	-	-	-	-	-	-	-	-
A-0-12	8	Calib	-	-	-	-	-	-	-	-	-
A-0-12	13	Calib	-	-	-	-	-	-	-	-	-
A-0-12	18	Calib	-	-	-	-	-	-	-	-	-
A-0-12	24	Calib	-	-	-	-	-	-	-	-	-
A-0-13	3	Meas	4077.6	105.8	1985.9	749.0	83.6	665.4	0°	0.3°	-0.30°
A-0-14	4	Meas	4337.6	105.8	2115.9	1023.5	83.6	939.9	+0.47°	0.3°	-0.17°
A-0-15	19	Meas	3413.7	105.8	1654.0	143.5	83.6	59.9	+2.80°	0.3°	+2.50°
A-0-16	20	Meas	3398.3	105.8	1646.3	233.6	83.6	150.0	+5.65°	0.3°	+5.35°
A-0-17	21	Meas	3428.8	105.8	1661.5	325.8	83.6	242.2	+8.40°	0.3°	+8.10°
A-0-18	22	Meas	3496.3	105.8	1695.3 nsec	595.1	83.6	511.5 nsec	+15.20°	0.3°	+14.90°

1. $\tau_2' = \dfrac{\tau_2 \text{ (MEAS)} - \tau_2 \text{ (BIAS)}}{2}$

2. $\tau_D' = \tau_D \text{ (MEAS)} - \tau_D \text{ (BIAS)}$

3. $\eta' = \eta\text{(MEAS)} - \eta\text{(BIAS)}$

Table 4-5. RTT-1 Range/Deflection Measurement Results

Location Code	Test No.	Function	R_d(Comp)	R_d(Surv)	Range Error (ft)	ϵ (θ_y)	Deflection Error
A-0-0	-	Not Used	-	-	-	-	-
A-0-1	5	Meas	1707.1	1623.0	+84.1	0.17°	+4.8 ft
A-0-2	6	Meas	1672.6	1623.0	+49.6	0.3°	+8.68 ft
A-0-3	7	Meas	1658.1	1623.0	+35.1	0.16°	+4.5 ft
A-0-4	9	Meas	1609.5	1623.0	-13.5	0°	0 ft
A-0-5	10	Meas	1585.2	1623.0	-36.8	0°	0 ft
A-0-6	11	Meas	1523.0	1623.0	-100.0	0°	0 ft
A-0-6	25	Meas Rep	1602.3	1623.0	-20.7	0°	0 ft
A-0-7	12	Meas	1582.5	1623.0	-40.5	0.15°	+4.1 ft
A-0-8	14	Meas	1669.5	1623.0	+46.4	0°	0 ft
A-0-9	15	Meas	1639.3	1623.0	+16.3	0°	0 ft
A-0-10	16	Meas	1650.0	1623.0	+27.0	0°	0 ft
A-0-11	17	Meas	1636.6	1623.0	+13.6	0°	0 ft
A-0-12	1	Calib	-	-	-	-	-
A-0-12	2	Calib	-	-	-	-	-
A-0-12	8	Calib	-	-	-	-	-
A-0-12	13	Calib	-	-	-	-	-
A-0-12	18	Calib	-	-	-	-	-
A-0-12	24	Calib	-	-	-	-	-
A-0-13	3	Meas	1625.6	1623.0	+2.6	0°	0 ft
A-0-14	4	Meas	1618.5	1623.0	-4.5	0°	0 ft
A-0-15	19	Meas	1640.0	1623.0	+17.1	0°	0 ft
A-0-16	20	Meas	1622.9	1623.0	-0.1	0°	0 ft
A-0-17	21	Meas	1625.9	1623.0	+2.9	0°	0 ft
A-0-18	22	Meas	1593.0	1623.0	-30.0	0°	0 ft

$$R_d(\text{Comp}) = c\dot{\tau}_D \left(\frac{2\tau_2' \cos \eta + \tau_D}{2\tau_2' - \tau_D'} - \right)^{-1}$$

Table 4-6. Measured vs Analytically Projected Range Errors

Location Code	Test No.	Function	(1) ΔR_d	(2) σR_d	Comments
A-0-0	-	Not Used	-	-	
A-0-1	5	Meas	+84.1	104.6	
A-0-2	6	Meas	+49.6	105.0	
A-0-3	7	Meas	+31.5	104.9	
A-0-4	9	Meas	-13.5	36.2	
A-0-5	10	Meas	-36.8	36.8	
A-0-6	11	Meas	-100.0	37.3	$\Delta R_d > 2\sigma R_d$
A-0-6	25	Meas Rpt	-20.7	37.3	
A-0-7	12	Meas	-40.5	38.2	$\Delta R_d > 1\sigma R_d$
A-0-8	14	Meas	+46.4	25.3	$\Delta R_d > 1\sigma R_d$
A-0-9	15	Meas	+16.3	25.4	
A-0-10	16	Meas	+27.0	25.6	$\Delta R_d > 1\sigma R_d$
A-0-11	17	Meas	+13.6	26.0	
A-0-12	1	Calib	-	-	
A-0-12	2	Calib	-	-	
A-0-12	8	Calib	-	-	
A-0-12	13	Calib	-	-	
A-0-12	18	Calib	-	-	
A-0-12	24	Calib	-	-	
A-0-13	3	Meas	+2.6	23.1	
A-0-14	4	Meas	-4.5	23.1	
A-0-15	19	Meas	+17.1	23.1	
A-0-16	20	Meas	-0.1	36.5	
A-0-17	21	Meas	+2.9	36.9	
A-0-18	22	Meas	-30.0	38.1	
					14 Measurements were within 1σ 17 Measurements were within 2σ 18 Measurements were within 3σ

1. Observed Range Error
2. Computed Range Error

Table 4-7. RTT-1 Link S/N Levels and Noise-Induced Measurement Error Calculation Results

Location Code	Test No.	Function	S/N(R-BS)	S/N(V-R)	S/N(I-R)	S/N(I-BS)	S/N(V-BS)
A-0-0	-	Not Used	-	-	-	-	-
A-0-1	5	Meas	+25.6	+101.2	+44.1	+90.5	+81.3
A-0-2	6	Meas	26.2	87.1	44.7	+90.5	81.3
A-0-3	7	Meas	27.0	76.4	45.5	+90.5	81.3
A-0-4	9	Meas	25.0	75.6	43.5	+90.5	81.3
A-0-5	10	Meas	25.0	62.1	43.5	+90.5	81.3
A-0-6	11	Meas	24.8	54.2	43.3	+90.5	81.3
A-0-6	25	Meas Rep	-	-	-	-	-
A-0-7	12	Meas	24.3	46.7	43.0	+90.5	81.3
A-0-8	14	Meas	24.8	67.6	43.3	+90.5	81.3
A-0-9	15	Meas	23.9	56.0	42.3	+90.5	81.3
A-0-10	16	Meas	23.2	48.3	41.7	+90.5	81.3
A-0-11	17	Meas	22.4	41.6	40.8	+90.5	81.3
A-0-12	1	Calib	23.3	51.9	41.7	+90.5	81.3
A-0-12	2	Calib	-	-	-	-	-
A-0-12	8	Calib	-	-	-	-	-
A-0-12	13	Calib	-	-	-	-	-
A-0-12	18	Calib	-	-	-	-	-
A-0-12	24	Calib	-	-	-	-	-
A-0-13	3	Meas	21.9	41.4	40.4	+90.5	81.3
A-0-14	4	Meas	20.7	35.3	39.2	+90.5	81.3
A-0-15	19	Meas	25.1	78.8	43.5	+90.5	81.3
A-0-16	20	Meas	25.0	66.4	43.5	+90.5	81.3
A-0-17	21	Meas	24.9	59.4	43.4	+90.5	81.3
A-0-18	22	Meas	24.5	47.2	43.0	+90.5	81.3
			db	db	db	db	db

m = 24.3	m = 60.6	m = 42.8	m = 90.5	m = 81.3	
σ_τ = 2.2 ns	σ_τ = 0.03 ns	σ_τ = 0.26 ns	σ_τ = 0.001 ns	σ_τ = 0.003 ns	one-pulse τ's.
σ_τ = 0.36°	NA	NA	NS	τ_θ = 0.00008°	

where

σ_η = Standard Deviation (S.D.) in measuring $\eta = \theta_V - \theta_R$

$\sigma_{\theta_V}(N)$ = S.D. in measuring θ_V due to S/N condition.

= 0.00008° (1 pulse)

$\sigma_{\theta_V}(M)$ = S.D. in measuring θ_V due to multipath effects.

= 0.89° (1 pulse)

$\sigma_{\theta_R}(N)$ = S.D. in measuring θ_R due to S/N condition.

= 0.36° (1 pulse)

$\sigma_{\theta_R}(M)$ = S.D. in measuring θ_E due to multipath effects.

= 3.18° (1 pulse)

σ_{SYS} = S.D. in measurement process due to other random system error sources.

= 0.14° (1 pulse)

For the analysis leading to the above results, see Appendix A.1.

σ_τ Considerations

The standard deviation in TOA and TDOA measurements identified in Table 4-3 were 18.2 msec and 29.6 nsec, respectively. These should relate to subcomponent values as follows:

$$\sigma_{TOA} = \sqrt{\sigma_\tau^2(SYS) + \sigma_\tau^2(I\text{-}BS) + \sigma_\tau^2(I\text{-}R) + \sigma_\tau^2(R\text{-}BS)} \qquad (4\text{-}2)$$

(180 pulse pairs)

$$\sigma_{DTOA} = \sqrt{\sigma_\tau^2(SYS) + \sigma_\tau^2(V\text{-}BS) + \sigma_\tau^2(V\text{-}R) + \sigma_\tau^2(R\text{-}BS)} \qquad (4\text{-}3)$$

(360 pulse pairs)

where

σ_{TOA} = Standard deviation (S.D.) in measuring time difference between reference pulse coupled by cable from interrogator and pulse from repeater in response to interrogator.

σ_{DTOA} = S.D. in measuring time difference for receipt of victim radar pulse via direct radiation to base station and via victim radar - repeater - base station route.

$\sigma_\tau(SYS)$ = S.D. in measurement process of base station equipment.

= 64 ns

$\sigma_\tau(I\text{-}BS)$ = S.D. component introduced by interrogator to base station link.

= 0 ns

$\sigma_\tau(I\text{-}R)$ = S.D. component introduced by interrogator to repeater link.

= 64 ns

$\sigma_\tau(R\text{-}BS)$ = S.D. component introduced by repeater to base station link.

= 228.5 ns

$\sigma_\tau(V\text{-}BS)$ = S.D. component introduced by victim radar to base station link.

= 64 ns

$\sigma_\tau(V\text{-}R)$ = S.D. component introduced by victim radar to repeater link.

= 504.2 ns

For the analysis leading to the above results see Appendix A.2.

4.1.5 Extrapolation of Results In Range

The field tests were conducted employing a victim radar to base station range (Rd) of 1623 feet. All values of R_1, R_2 and ΔR employed during tests were scaled to correspond to operation at a victim radar to base station range of approximately 15 kilometers. Also, the RTT-1 links were padded with RF attenuators to approximate the S/N conditions for 15 kilometer range operation.

To extrapolate the results obtained during the field tests to a 15 kilometer range, it is merely necessary to introduce the proper range multiplication factor into the equations identifying RTT-1 system errors.

In the case of RTT-1 system deflection error, this is readily accomplished. Deflection error is given by the equation:

$$\sigma_{DEFL} = R_d \sigma_{\theta_V} \tag{4-4}$$

The deflection error will increase proportionally with range. At 15 kilometers, the expected deflection error will be 23.3 meters.

Extrapolation of the RTT-1 range error is less straightforward. Equation (2-2) can be rewritten as:

$$\sigma(R_d) = \sqrt{\left\{\frac{2R_d^2\ [(\Delta R) + 2R_2\ (1 - \cos\eta\ )\ (R_2 - \Delta R)]}{(\Delta R)^2\ (2R_2 - \Delta R)^2}\ \sigma_{\Delta R}\right\}^2 + \left\{\frac{2R_d^2\ (\Delta R)^2\ (1 + \cos\eta\ )\ \sigma R_2}{(\Delta R)^2\ (2R_2 - \Delta R)^2}\right\}^2 + \left\{\frac{2R_d^2\ [\Delta R(2R_2 - \Delta R)\ R_2 \sin\eta\ ]\sigma_\eta}{(\Delta R)^2\ (2R_2 - \Delta R)^2}\right\}^2} \tag{4-5}$$

showing σ (Rd) to be the RSS product of three components. The components are functions of $\sigma_{\Delta R}$, σ_{R_2} and σ_η where $\sigma_{\Delta R}$ and σ_{R_2} are the time domain counterparts of σ_{DTOA} and σ_{TOA}.

Examination of these components reveals that those associated with $\sigma_{\Delta R}$ and σ_{R_2} (or, conversely σ_{DTOA} and σ_{TOA}) do not vary as a function of range. The component associated with σ_η, however, varies directly with range. An illustration of this is given in Figure 4-2. The geometry associated with field test situation A-0-16 is used. The left side of the curves represents the field test range (1623 feet). The right side of the curves corresponds to a base station to victim radar range of 15 kilometers. It is seen that during the field tests, the three variant quantities (i.e., σ_η, σ_{TOA} and σ_{DTOA}) each contribute significantly to the overall range error (σ_{Rd}). At ranges in excess of four kilometers, the σ_η component dominates the overall error. The angle η in this example case is greater than three degrees.

The performance of the RTT-1 system, extrapolated in range, based upon the measured values of σ_{OTA}, σ_{DTOA} and σ_η, is shown in Figure 4-3. The 14.8 kilometer point along the ordinate represents the location of the victim radar.

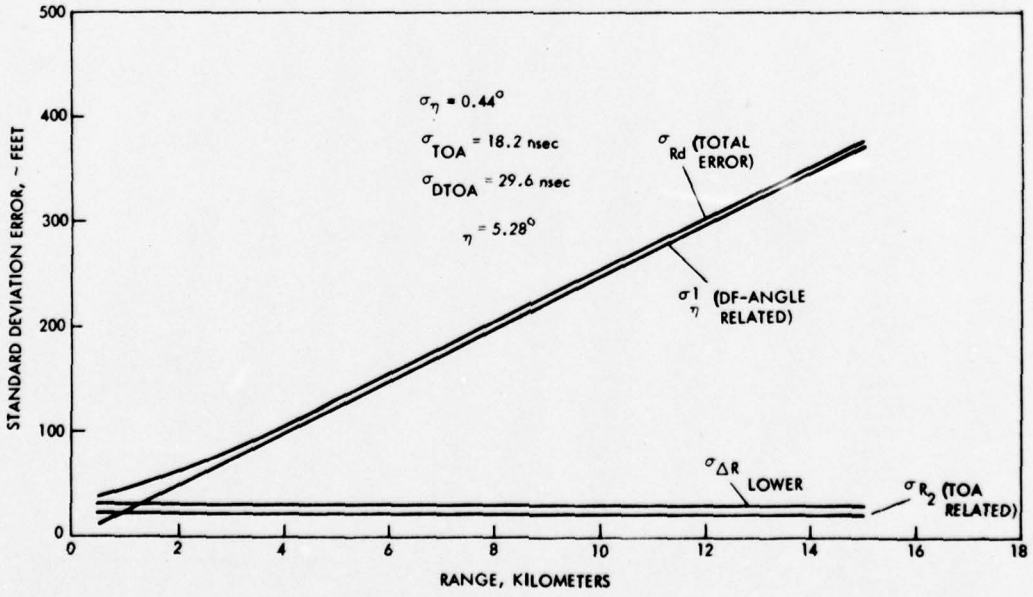

Figure 4-2. Standard Deviation Error vs. Target Range

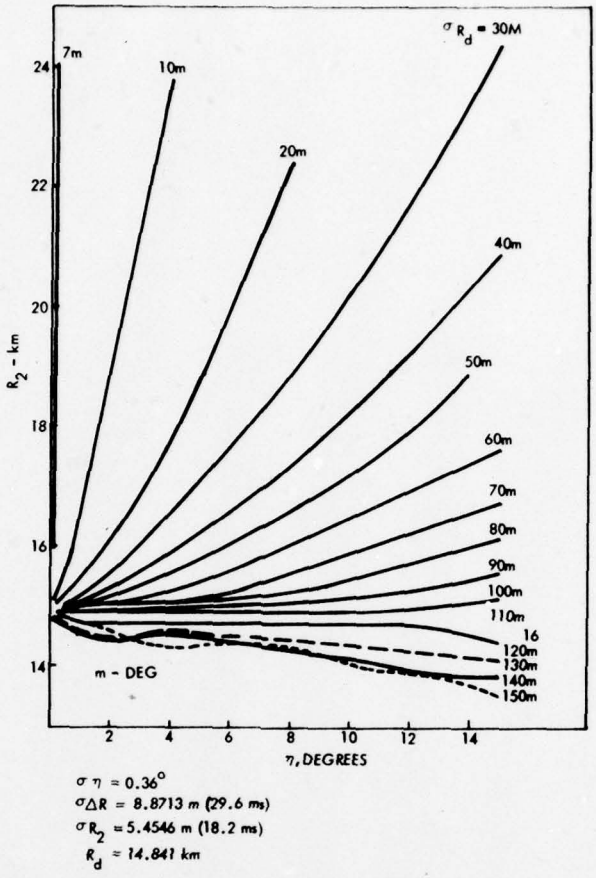

Figure 4-3. RTT-1 Performance at 14.8 km Range

Ordinate values (R_2) represent repeater range from the base station. Abscissa values represent η, here the repeater angle offset from the victim radar. Performance is shown in terms of contours of constant value of σ_{R_d}.

If one assumes that σ_{R_d} = 40 m is the maximum tolerable range error, then the repeater must be located between the σ_{R_d} = 40 meter contour and the abscissa (or in the mirror image region on its opposite side) and within the dotted line signifying victim radar to repeater link S/N limit.

The accuracy obtained along the ordinate, 7 meters, represents the DTOA performance of the system.

At repeater locations between the victim radar and the base station (for the given span of values of η) system operation is not feasible.

4.2 FOLIAGE OBSTRUCTION EFFECTS EXAMINATION RESULTS

4.2.1 Data Reduction Approach

The approach used in examining foliage obstruction effects was that of comparing two geographically similar test situations, one of which was free of foliage obstruction and the other containing a quantifiable element of it. The test results of the two cases were then compared and analyzed to identify relevant physical phenomena and assess their impact. Four such pairs of tests were conducted.

In general, the results of foliage obstruction were negative (regarding RTT-1 operability) and dramatic with one or more of the RTT-1 links ceasing to operate. When this occurred, range compensation attenuation was reduced in an attempt to restore operation. The amount of attenuation extracted provided a mechanism to estimate the amount of foliage obstruction attenuation involved.

4.2.2 Measurement Results

Table 4-8 lists the surveyed range and angle parameters associated with the four pair of test situations used to examine foliage obstruction effects.

A-0-14/A-0-14' Tests - Table 4-9 lists the results of tests conducted for test situations A-0-14 and A-0-14'. These tests were unusual in that operation was possible in the presence of foliage obstruction. It is noted that interrogation of the repeater during A-0-14' tests was possible only after the range compensation attenuation in the repeater was reduced from 30 dB to 10 dB. Table 4-7 (test situation A-0-14) indicates that the S/N ratio in this link at these ranges is approximately 39.2 dB.

The repeater at station 14' was located immediately adjacent to a wall of foliage so that propagation was only possible via foliage penetration. Foliage penetration attenuation may be approximated by the relationship:

$$\alpha\,(\text{dB/foot}) = 0.0004\ f^{0.77}$$

Table 4-8. Surveyed Range/Angle Parameters for Foliage Obstruction Tests

Location Code	Test No.	Function	R_1 (ft)	R_2 (ft)	Rd (ft)	ΔR (ft)	θv (deg)	θR (deg)	η (deg)
A-0-14	4	Reference	470.0	2093.2	1623.0	940.0	0°	-0.008	-0.008
A-0-14'	23	Test	489.1	2081.0	1623.0	947.1	0°	+5.34	+5.34
20-26-27	26	Reference	435.0	8423.0	7988.0	870.0	0	0	-
20-26-30	27	Test	130.0	8072.2	7988.0	213.6	0	+0.71°	+0.71
20-26-30'	30	Reference	74.5	8088.3	8081.8	81.0	0	-0.53	-0.53
20-26-29	29	Test	130.3	8072.2	7988.0	213.6	0	-0.71	-0.71
20-30'-30"	28	Reference	75.7	8084.1	8076.3	93.5	+0.37	-0.15	-0.52
20-30-29	31	Test	199.2	8072.2	8072.2	199.2	-0.72°	+0.72	+1.42

where α is in MHz.

For transmission through fifty feet of foliage at 16 GHz, about 34.6 dB of attenuation is introduced. This produces a link S/N ratio sufficient to make the repeater inoperable.

Reduction of the range compensation attenuation by 20 dB restored the link S/N ratio of 24.6 dB and operation became possible.

Although the repeater to base station link is geometrically identical, it operated satisfactorily. Table 4-7 shows the unobstructed S/N ratio in this link to be of the order of only 20.7 dB. The foliage attenuation at 1500 MHz however, is only 5.6 dB, resulting in a net link S/N ratio of 15.1 dB. This is adequate for link operation.

Table 4-9. A-0-14/A-0-14' Test Results

Parameter	Units	Reference Location A-0-14	Test Location A-0-14'
τ_2	nsec	4337.6	4498.9
τ_2(Bias)	nsec	105.8	105.8
τ_2'	nsec	2115.9	2196.1
R_2(Calc)	ft	2080.5	2159.8
R_2(Surv)	ft	2093.0	2093.0
$\epsilon(R_2)$	ft	-12.5	+66.8
τ_D	nsec	1022.5	1102.5
τ_D(Bias)	nsec	83.6	83.6
τ_D'	nsec	939.9	1018.9
ΔR(Calc)	ft	924.2	1001.9
ΔR(Surv)	ft	940.0	940.0
$\epsilon(R_2)$	ft	-15.8	+61.9
η	deg	0	5.4
η(Bias)	deg	0.3	0.3
η'	deg	-0.3	5.1
η(Surv)	deg	0.008	5.34°
$\epsilon(\eta)$	deg	-0.29°	-0.24°
R_d(Calc)	ft	1618.5	1672.7
R_d(Surv)	ft	1623	1623.0
ϵ(Range)	ft	-4.5	+49.7
σ(Range)	ft	23.1	23.3
θ_v(DF)	deg	0.78°	-
θ_v(Opt)	deg	0.78°	-
$\epsilon(\theta_v)$	deg	0°	-
ϵ(Defl)	ft	0	-
∇(Defl)	ft	2.5	-

Notes Re A-0-14'

1. Atten. in I-R link reduced from 30 dB to 10 dB to achieve interrogation.
2. Approx. 50 feet foliage in I-R/R-BS link
3. Some thin foliage in V-R link. LOS was possible.

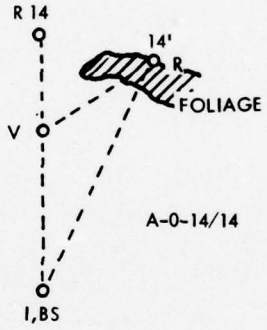

The victim radar to repeater link was only partially obstructed by foliage (of the order of 3 feet in aggregate). The attenuation here would be expected to be only 2 dB. It exhibited no discernible effect on link operability.

The overall impact of foliage obstruction on system performance can be examined by comparing the results obtained in the two cases. The measured value for τ_2 and τ_D (corresponding to R_2 and Δ_R) were increased. The values measured for Δ_R exhibited similar error in both cases. The RTT-1 range measurement error was 49.7 feet as opposed to a predicted error of 23 feet at this location.

These errors are symptomatic of delays introduced in the V-R and R-BS links. The mechanism of delay introduction is believed to be a combination of pulse shape distortion, i.e., degradation of leading edge slope due to interfoliage multipath and a signal strength-induceded variation in repeater delay.

20-26-27/20-26-30 Tests - Table 4-10 lists the results of tests conducted for test situations 20-26-27 and 20-26-30. During these tests, foliage obstruction made repeater interrogation impossible. It was, however, possible to measure τ_D, indicating that the 1500 MHz repeater to BS through the same foliage was operative.

The S/N condition at the repeater at station 30 in the absence of foliage is -45 dB (including the effect of 15 dB of range compensation attenuation). For the conditions existent, the attenuation due to foliage obstruction would be approximately 89.8 dB. It is interesting to compare this to the attenuation which would result from diffraction over the tree line. The latter may be approximated using the empirical expression described by Harvey and determined to be 42.4 dB. Clearly, if propagation were to take place, it would be via diffraction. Using the latter level of attenuation, link S/N becomes -3.2 dB. Extraction of range compensation improves this to +11.8 dB, approximately the threshold of operability. Given the variance associated with the empirical attenuation estimates, it is reasonable that the link was inoperative.

The S/N ratio at the base station resulting from repeater radiation is calculated to be 44.8 dB, including the effects of range compensation attenuation at the base station. Foliage penetration at 1500 MHz would produce attenuation of

Table 4-10. 20-26-27/20-26-30 Test Results

Parameter	Units	Reference Location 20-26-27	Test Location 20-26-30	
τ_2	nsec	17228.5	-	Notes Re 20-26-30
τ_2(Bias)	nsec	105.8	105.8	1. Atten. in I-R link reduced from 15 dB to 4 dB, to 0 dB. Could not interrogate.
τ_2'	nsec	8561.4	-	
R_2(Calc)	ft	8418.2	-	2. Tree line, 50 ft. high, 130 ft. thick in I-R/R-BS link.
R_2(Surv)	ft	8423.0	8072.2	
$\epsilon(R_2)$	ft	-4.8	-	
τ_D	nsec	963.7	335.3	
τ_D(Bias)	nsec	83.6	83.6	
τ_D'	nsec	880.1	251.7	
ΔR(Calc)	ft	865.4	247.5	
ΔR(Surv)	ft	870.0	213.6	
$\epsilon(R_2)$	ft	-4.6	+33.9	
η	deg	0	0.25	
η(Bias)	deg	-	+0.3	
η'	deg	0	-0.05	
η(Surv)	deg	0	+0.71	
$\epsilon(\eta)$	deg	-	-0.76	
Rd(Calc)	ft	7985.6	-	
R_d(Surv)	ft	7988.0	7988.0	
ϵ(Range)	ft	-2.4	-	
σ(Range)	ft	23.1	-	
θ_v(DF)	deg	-	-	
θ_v(Opt)	deg	-	-	
$\epsilon(\theta_v)$	deg	-	-	
ϵ(Defl)	ft	-	-	
∇(Defl)	ft	-	-	

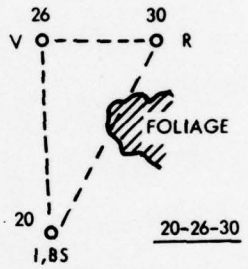

14.5 dB. Diffraction attenuation at this frequency would result in approximately 27 dB. Foliage penetration is, therefore, the probable mode of propagation. The net S/N ratio for link R-BS then is +30.3 dB.

The introduction of foliage obstruction into link R-BS resulted in an increase in the error in measuring R from -4.6 feet (situation 20-26-27) to +33.9 feet (situation 20-26-30). The error is symptomatic of increased delay in the R-BS link due to pulse distortion and increased repeater delay due to signal attenuation.

20-26-30'/20-26-29 Tests - Table 4-11 lists the results of tests conducted for situations 20-26-30' and 20-26-29. Here, attempts were made to interrogate and receive responses from the repeater only. This was achieved under line of sight conditions with the repeater at site 30', but was not possible at site 29.

The obstruction to the I-R link at site 29 was a forested hill, approximately 80 feet in height (up to the tree line) and 300 feet thick. Diffraction attenuation along the tree line would amount to an estimated 55.3 dB resulting in an S/N ratio at the repeater of -1.2 dB.

20-30'-31"/20-30-29 Tests - Table 4-12 lists the results of tests conducted for situations 20-30'-30" and 20-30-29. For operation in the former situation, all links were LOS. For the latter, neither repeater nor victim radar enjoys unobstructed LOS to the base station.

Interrogation of the repeater was not possible for the reasons discussed on the preceding page, however, measurement of the difference in time of arrival (and subsequency computation of ΔR) was possible when the victim radar antenna was directed toward the base station.

Under these conditions, the unobstructed-view S/N ratio for the V-BS link would be 87.1 dB. The introduction of 55.3 dB of tree line diffraction attenuation leaves a net S/N ratio of 31.9 dB. Link operation via minor lobe radiation (40 dB lower) was not possible.

Table 4-11. 20-26-30'/20-26-29 Test Results

Parameter	Units	Reference Location 20-26-30'	Test Location 20-26-29	
τ_2	nsec	16536.4	-	Notes Re 20-26-29
τ_2(Bias)	nsec	105.8	105.8	1. Atten. in I-R link reduced from 15 dB to 0 dB. Could not interrogate.
τ_2'	nsec	16430.6	-	
R_2(Calc)	ft	8078.0	-	2. Trees on hill, total height 80 ft., 300 ft. thick in I-R/R-BS link.
R_2(Surv)	ft	8088.3	8072.2	
$\epsilon(R_2)$	ft	-10.3	-	
τ_D	nsec	-	-	
τ_D(Bias)	nsec	-	-	
τ_D'	nsec	-	-	
ΔR(Calc)	ft	-	-	
ΔR(Surv)	ft	-	-	
$\epsilon(R_2)$	ft	-	-	
η	deg	-	-	
η(Bias)	deg	-	-	
η'	deg	-	-	
η(Calc)	deg	-	-	
η(Surv)	deg	-	-	
$\epsilon(\eta)$	deg	-	-	
R∂(Calc)	ft	-	-	
R_d(Surv)	ft	-	-	
ϵ(Range)	ft	-	-	
σ(Range)	ft	-	-	
θ_v(DF)	deg	-	-	
θ_v(Opt)	deg	-	-	
$\epsilon(\theta_v)$	deg	-	-	
ϵ(Defl)	ft	-	-	
∇(Defl)	ft	-	-	

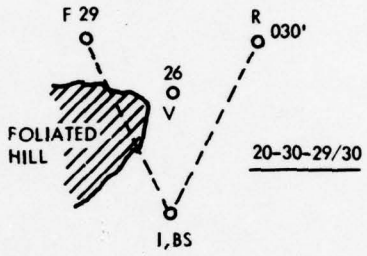

Table 4-12. 20-30'30"/20-30-29 Test Results

Parameter	Units	Reference Location 20-30'-30"	Test Location 20-30-29
τ_2	nsec	16572.6	-
τ_2(Bias)	nsec	105.8	83
τ_2'	nsec	8233.4	-
R_2(Calc)	ft	8095.8	-
R_2(Surv)	ft	8094.1	8072.2
$\epsilon(R_2)$	ft	+1.7	-
τ_D	nsec	164.5	244.5
τ_D(Bias)	nsec	83.6	83.6
τ_D'	nsec	80.9	160.9
ΔR(Calc)	ft	79.5	158.2
ΔR(Surv)	ft	93.5	199.2
$\epsilon(R_2)$	ft	-14.0	-41.0
η	deg	-0.55	-0.2
η(Bias)	deg	+0.30	0.30
η'	deg	-0.35	-0.5
η(Surv)	deg	-0.52	+1.42
$\epsilon(\eta)$	deg	+0.17	-1.92
$R\partial$(Calc)	ft	8072.3	-
R_d(Surv)	ft	8076.3	8072.2
ϵ(Range)	ft	-4.0	-
σ(Range)	ft	49.7	-
θ_v(DF)	deg	-	-
θ_v(Opt)	deg	-	-
$\epsilon(\theta_v)$	deg	-	-
ϵ(Defl)	ft	-	-
∇(Defl)	ft	-	-

Notes Re 20-30-29

1. Atten. in V-BS link removed. Could only receive when victim radar pointed toward base station.
2. Atten. in I-R link removed. Could not interrogate.
3. Trees on hill, total height 80 ft., 300 ft. thick in V-BS link.
4. Tree line 50 ft. high, 120 ft. thick in I-R/R-BS link.

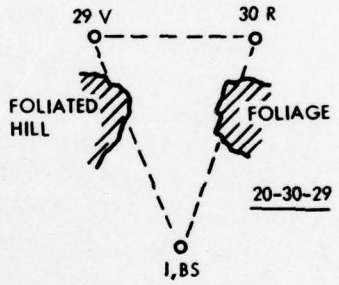

Under these conditions, the computed value of ΔR was 41 feet less than the surveyed value. In preceding measurements, the error had been on the positive side. The reason, of course, is that τ_D is measured by taking the difference between direct victim radar radiation, and repeated radiation. In effect, the victim radar pulse starts the time measurement and the repeated pulse ends it. In preceding tests, the delay was only in the repeater loop; hence, an apparent increase in τ_D. In this case, a greater delay was in the direct path, producing a reduction in the measured value for τ_D.

As in the preceding cases, the increase in path length due to diffraction does not account for the variation in delay. This must be attributed to pulse shape (leading edge) distortion.

The measured value for η differed from the surveyed value by 1.42°. It was noted that both target signals were the result of diffracted propagation.

18-X-21 Situation Test Results - This brief series of tests had as their objective the isolation of terrain obstruction effects as the primary error contribution, and examination of the errors produced. The test range segment used was one in which the LOS path between base station, repeater and victim radar locations was obstructed by relatively clear earth. Between locations 18 (base station) and 21 (repeater), a series of measurements were made wherein attenuation levels in the I-R and R-BS links were varied to examine the impact of signal level on the terrain-distorted pulses resulting from diffraction propagation.

The data collected during 18-X-21 series tests is presented in Table 4-13. Also provided are the results of calculations at the base station link (R-BS) receiver input and at the link (I-R) repeater input. The following results are noted.

For a constant S/N ratio of 27.9 dB at the base station receiver in the (R-BS) link, a reduction of S/N of five dB (from 27.9 to 22.9) in the (I-R) link resulted in an increase in the measured TOA of from 6565.9 nsec to 6569.6 nsec or of 3.7 nsec. The corresponding error sensitivity is 0.74 nsec per dB in this (I-R) link.

Table 4-13. 10-X-21 Situation Test Results

Situation Test No.		18-X-21 82	18-X-21 33	18-X-21 33'	18-X-21 34
B.S. Loc.		18	18	18	18
R Loc.		21	21	21	21
τ_2	(nsec)	6565.9	6533.6	6569.6	-
τ_2(bias)	(nsec)	105.8	105.8	105.8	-
τ_2'	(nsec)	3230.1	3213.9	3231.9	-
R_2(Meas)	(ft)	3176.1	3160.2	3177.9	-
R_2(Surv)	(ft)	3164.6	3164.6	3164.6	3164.6
$\epsilon(R_2)$	(ft)	+11.5	-4.4	+13.3	-
L_{RC}(I-R)	(dB)	5	10	10	15
L_{RC}(R-BS)	(dB)	15	0	15	0
L_{DIFF}(I-R)	(dB)	29.3	29.3	29.3	29.3
L_{DIFF}(R-BS)	(dB)	23.0	23.0	23.0	23.0
S/N(R)	(dB)	+27.9	22.9	22.9	17.9
S/N(BS)	(dB)	+29.9	44.9	29.9	44.9

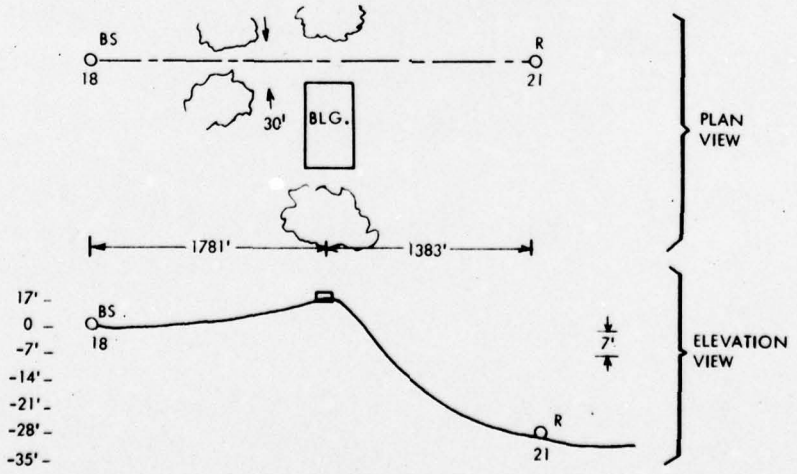

For a constant S/N ratio of 22.9 dB in at the repeater input of the (I-R) link, and S/N reduction of 15 dB (from 44.9 to 29.9) in the (R-BS) link produced an increased in TOA of from 6533.6 nsec to 6569.6 nsec, or of 35 nsec. The corresponding error sensitivity is 2.4 nsec per dB in this (R-BS) link.

It is noted that reduction of the S/N ratio to a calculated value of 17.9 dB in the (I-R) link resulted in link inoperability suggesting an error of the order of 10 dB, probably in the diffraction loss estimate. This is not unreasonable given the empirical nature of the calculation and the variability of diffraction effects.

The (R-BS) link error sensitivity of 2.4 nsec per dB implies substantial degradation of the repeater pulse rise time due to diffraction and suggests that the simple thresholding process used to start and stop time measurements in the RTT-1 test system may be inadequate when diffracted transmission paths are encountered.

18-21-22 Situation Test Results - An attempt to measure DTOA with the base station located at station 18, the victim radar located at station 21 and the repeater located at station 22 (612 feet beyond, and in line with station 21) produced substantial measurement error. Attempts to correlate DF and theodolite measurements suggested that signal reception was from other than the diffracted straight-line path along which the RTT-1 elements were located.

The manner in which trees and a building "pinched" the test range between sites 18 and 21 near the crown of the hill, suggests the presence of propagation moding effects and the presence of peaks and nulls which that implies. The presence of metal in the building would also impact the composite propagation situation under these conditions.

There obviously exist propagation conditions under which systems relying on ground-ground transmission of signals will not function properly. Situation 18-21-22 is one of these.

SECTION 5

SECTION 5
CONCLUSIONS

Based upon the results obtained during this investigation, conclusions regarding RTT-1 technical feasibility and applicability to U.S. Army needs may be formulated.

5.1 TECHNICAL FEASIBILITY

The RTT-1 field test system performed in essential accordance with the predictions of the analytical model. The tests and subsequent data analysis did, however, produce evidence that the following effects were present during test system operation:

- Multipath from diffuse scatters in the vicinity of RRT-1 system elements.
- Signal attenuation and distortion due to thick foliage and terrain obstructions in the various RTT-1 links.
- Specular multipath from discrete scatterers a distance from the vicinity of RTT-1 system elements.

In general, it was possible to isolate these effects and examine their impact independently.

5.1.1 Diffuse Multipath Effects

Under line of sight or near line of sight conditions for all of the RTT-1 links, the primary disruptive influence upon system operation was multipath from diffuse scatterers in the vicinity of the system elements. Its mechanism of impact in the time measurement process is degradation of pulse rise time. The effect produced is that of increasing the apparent delay in the pertinent links. The result produced on system operation is an increase in TOA and an increase or decrease in DTOA, depending upon which link is most severely affected.

The mechanisms of impact in the DF process were operator confusion in separating direct from multipath responses on the display. The effect produced was a smearing of the DF null. The result produced on system operation is a noise-like degradation in DF accuracy.

Due to the general noise-like quality of diffuse multipath effects, it was possible to consider them an independent random process insofar as system operation was concerned. Doing this, the following conclusions may be drawn.

1. Random multipath from diffuse scatterers represents the most significant source of error in RTT-1 system performance. In vulnerable links, its contribution exceeds those of internal noise by factors of the order of 100:1.
2. The relative impact of diffuse multipath in a given link is strongly dependent upon the directivity of the antennas at the link terminals. The RTT-1 link exhibiting the greatest vulnerability to diffuse multipath was that from the victim radar antenna's minor lobes to the omnidirectional repeater antenna.
3. The behavior of diffuse multipath-induced errors was statistically well-behaved. "Mean" components represented consistent system biases and were successfully extracted. "Random" components were reducible via integration of samples, the improvement being generally proportional to the square root of the number of samples integrated. This held for both time and DF measurement processes.
4. The nominal time measurement error standard deviation was of the order of 22.6 nsec. This produced a corresponding range error standard deviation of approximately seven meters when the base station, victim radar, and repeater were aligned.
5. The nominal angle measurement error standard deviation was of the order of 0.36 degrees and was due primarily to errors in the 1500 MHz repeater - base station link DF process. This represents the dominant range error source in the RTT-1 concept when it is employed at ranges of 4 km or greater.

6. The deflection (cross-track range) error of the RTT-1 concept is directly proportional to the accuracy of the DF process used at the victim radar's frequency. In the RTT-1 test system, this accuracy was better than 0.1 degrees. It would produce an expected deflection error of 26 meters at a range of 15 kilometers.

If operation of RTT-1 equipment under near line of sight conditions is intended, performance levels corresponding to those of the test system should prove adequate to produce location error standard deviations of less than 40 meters without prohibitively constraining repeater deployment. Substantial performance margin exists in the time measurement process; however, DF measurement capability must be considered critical in light of its proportionality to deflection error.

Figure 5-1 shows 40-meter range error standard distribution contours in a field representative of possible repeater locations near the victim radar. Contour 3 represents RTT-1 test system performance levels. The area above and to the left of the contour represents acceptable repeater deployment region. Contour 2 shows the impact of degrading the system's time measurement accuracy by a factor of

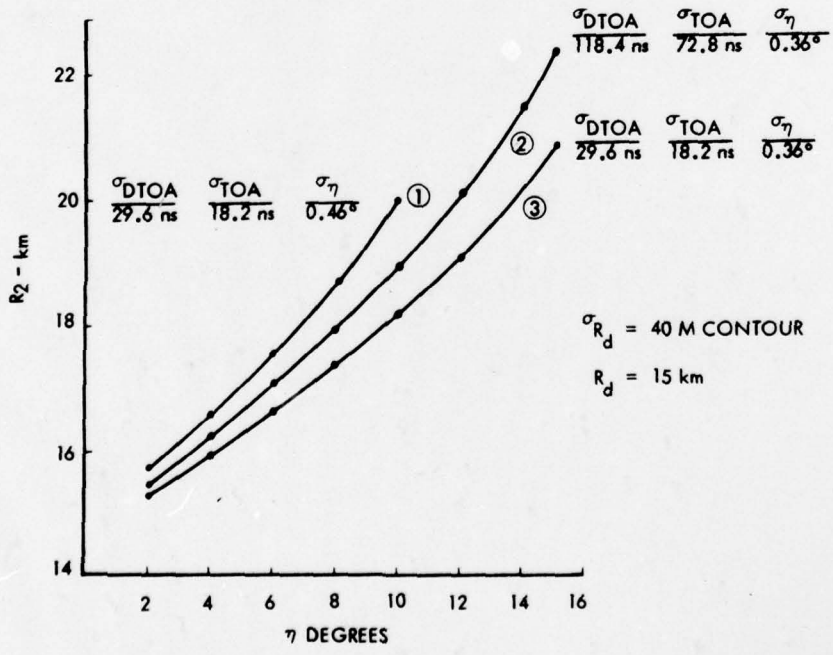

Figure 5-1. 40-Meter Range Error Standard Distribution Contours

four. It is seen that little constraint upon repeater location is introduced. Contour 1 shows the impact of increasing angle measurement error standard deviation from 0.36° to 0.46°. The results are negative and dramatic.

In general, examination of the RTT-1 test system in the presence of diffuse multipath under near line of sight conditions indicates that implementation of a system to operate in this manner is technically feasible.

5.1.2 Diffraction Due to Foliage and Terrain Obstruction

When any of the RTT-1 system links are obstructed by foliage or terrain, system operation is degraded in an analytically predictable manner. Given a knowledge of the obstruction, errors which are introduced should be compensatable. Extreme obstruction, however, will result in link (and, therefore, system) inoperability. Again, the result is analytically predictable.

Foliage obstruction at the 16,000 MHz victim radar and interrogator frequency resulted in link propagation by means of diffraction effects over the tree line. For the situations examined, this produced signal attenuation ranging from 22 to 52 dB. In the latter case, link S/N margins were exceeded and operation ceased.

Foliage obstruction at the 1500 MHz repeater frequency resulted in link propagation via foliage penetration. In the situations examined, this produced signal attenuation of the order of 10 dB or less and did not limit link operation.

Terrain obstruction at both link frequencies produced propagation by means of diffraction and concomitant signal attenuation. As in the case of foliage obstruction, the attenuation was predictable.

Where the obstruction was geometrically well behaved (a smooth ridge or tree line), little noticeable DF error was introduced. In general, sufficient S/N margin was available to support operation.

Operation through (or over) obstructions degraded time measurement accuracy. The principle of degradation was an increase in pulse rise time coupled with

attenuation. It produces an increase in apparent TOA and an increase or decrease in DTOA, depending upon which link is more severely affected.

The most serious effect noted (errors approaching one nsec/dB) involved the links terminating at the base station. This source of error can be mitigated if a different measurement technique than that employed in the RTT-1 test system is used.

The RTT-1 test system measured time between threshold crossings of first and second pulses. This is susceptible to leading edge distortion and signal attenuation effects. An alternative technique (albeit more complex) is to determine the mid-point between a pulse's 10 percent and 90 percent levels and use that as the measurement reference point. This practice could be expected to significantly reduce this source of system error.

In general, link failure occurs under these conditions due to S/N insufficiency in those links at the higher microwave frequencies.

5.1.3 Specular Multipath

When foliage or terrain obstructions block direct path propagation in RTT-1 links, the possibility of indirect path propagation via specular reflectors in the region increases. This can produce dramatic time and angle measurement errors in the RTT-1 process.

Specular multipath can be expected when non-line of sight conditions are coupled with severe terrain irregularity. It might also be produced by intentional ECCM operations.

Antenna directivity is the foremost RTT-1 protection against this source of error. The use of a first-pulse-in rule for time measurement processes affords protection. Appropriate ancillary displays can provide assistance in recognizing when specular multipath is present.

Although specular multipath can be a source of catastrophic error, resistance to it can be designed into a system and, when its effects are observed, operation can be discontinued.

5.1.4 Analytical Model Adequacy

The RTT-1 analytical model, upgraded to include the effects of multipath, should serve to predict adequately the performance of the RTT-1 concept when employed by a system comprised of equipments within the present technological state-of-the-art, in those situations in which they are presently expected to operate.

The effects of multipath experienced during RTT-1 field testing, it is recognized, constitute a small subset of the effects which might be encountered should world-wide deployment be contemplated. The results of Army tests of other ground-ground systems should provide a data base permitting broader examination of RTT-1 performance, should this be desired. Sufficient understanding of the problem exists to assimilate such information.

5.2 APPLICABILITY

A realistic appraisal of the applicability of the RTT-1 concept of U.S. Army needs must address itself, first, to what those needs are, and second, to what the RTT-1 offers in regard to them.

5.2.1 AN/MSQ-103 Augmentation

The essence of the RTT-1 concept is the use of remotely deployed repeaters in conjunction with a single ELINT-type base station to provide targeting-precision location information regarding hostile emitters. The Army is in the process of procuring the AN/MSQ-103, Teampack, ELINT system. The AN/MSQ-103 is expected to constitute an essential element in the Army's battlefield intelligence collection equipment inventory for the foreseeable future. It functions by providing recognition and line of bearing data on hostile emitters with its field of view.

The use of one or more repeaters with the AN/MSQ-103 to provide targeting information on selected emitters should meaningfully increase the utlity of that equipments in the field without significantly increasing the cost to the Army of acquiring or using it.

The results of the field tests, described herein, indicate that the provision of repeaters with the requisite capability are within the present technological state-of-the-art. Their achievable performance would be dictated by the capability inherent in the AN/MSQ-103 equipment itself and in the way in which the repeaters are employed. Two modes of repeater employment warrant discussion, based upon present RTT-1 understanding:

1. RPV-borne repeaters,
2. ground-located repeaters.

The use of RPV-borne repeaters offers the greatest potential for operational flexibility. This application of RTT-1 technology was cited by Maron[1] in his disclosure of the concept and subsequently examined by Rambo[2]. The present recognition that RPV-borne EW systems offer significant support to Army ground force elements provides currency to this application. RTT-1 technical feasibility test results offer substantiation.

An RPV-borne repeater mitigates the most significant error mechanisms noted during the field tests by assuring line of sight propagation between the most multipath-susceptible RTT-1 element (the repeater) and other system elements. This optimal propagation situation can be expected to be retained under virtually all topological situations. If the ELINT base station can detect a victim emitter, an RPV-borne repeater should permit its precise location.

Ground-located repeaters are susceptible to the error mechanisms experienced in the RTT-1 field tests; however, under two broad sets of conditions, their use warrants consideration. These are where the local topography exhibits relatively little foliage, and where the terrain is smooth (rolling hills as opposed to craggy horizon lines). In such locales, operation should be predictable and effective. Even under adverse terrain/foliage conditions, effective performance can be obtained if repeater locations can be predesignated, as in anticipation of retrograde maneuvers.

---

1. I. Maron, Advanced Program Concept: EXPELS, RCA/G&CS Memorandum, 27 February 1979.
2. W. Rambo, RPV in a Tactical EW Support Role, Tech. Report 2, Contract DAAB07-77-D-6388, April 1979.

The techniques being evolved in the Army's REMBASS program for the deployment of unattended ground sensors and repeaters are applicable to the deployments of RTT-1 repeaters. These include hand emplacement, helicopter deployment and artillery deployment mechanizations.

The use of rockets as repeater deployment mechanisms is also warranted. Ground-located repeaters need only be in the general proximity of victim systems. The precision of hand emplacement or artillery deployment is not a necessity.

5.2.2 Closed-Loop Targeting Techniques (RTT-2)

The feasibility of using remotely-deployed repeaters in accordance with RTT-1 processes suggests a technique for accurately guiding munitions toward hostile emitters despite the fact that they may have ceased transmission. The principles of this technique, designated for convenience RTT-2, are shown in Figures 5-2 and 5-3.

Figure 5-2, RTT-2 Approach, shows the essential elements of operation. A hostile emitter's radiations are intercepted by a minimum of three remotely-deployed repeaters at known locations in its vicinity. The radiations are relayed to an ELINT base station where the difference in times of arrival are measured and recorded.

The repeater-base station range contributions to the DTOA measurements are extracted, leaving time-difference factors, independent of base station location, which precisely locate the emitter in a coordinate system defined by the repeater locations. These time-difference factors may then be programmed into a weapon guidance package.

The weapon, a missile or harrassment RPV, for instance, would be launched toward the general location of the victim. While en route, it would emit pulses which are repeated by the remotely deployed units in exactly the same manner in which they repeated victim emitter pulses. These repeated pulses are received by the weapon guidance package whose function is to restore, by means of vehicle maneuvers, the time-difference factors identified by the base station.

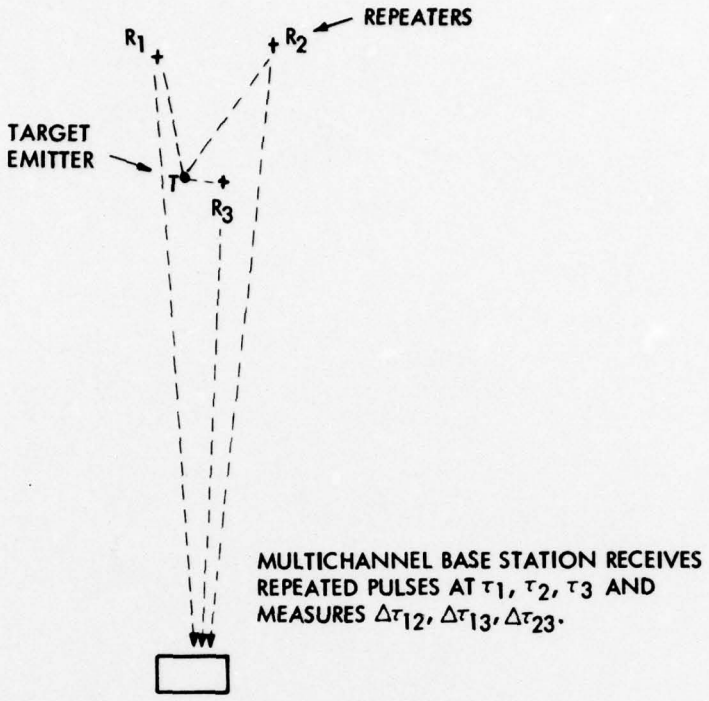

Figure 5-2. RTT-2 Approach

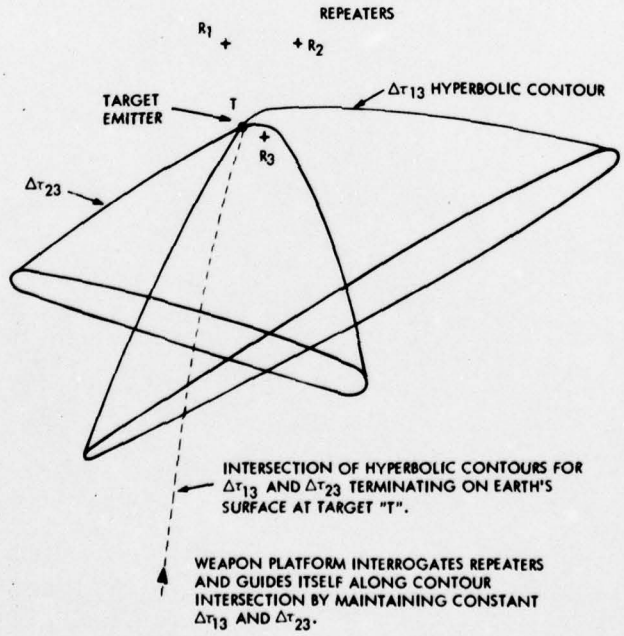

Figure 5-3. RTT-2 Guidance Contours

Figure 5-3, RTT-2 Guidance Contours, illustrates the principle. The three repeaters form two independent DTOA networks each of which describes a hyperbolic surface containing the victim emitter. The conjunction of the two surfaces is a line in space terminating at ground level on the victim emitter. The operation of the weapon guidance package is to intercept the spatial line and follow it to the victim emitter.

The airborne weapon mitigates much of the multipath difficulty identified during RTT-1 tests. Repeater location may be preselected in anticipation of retrograde maneuvers and in recognition of probable emitter locations. Link frequencies can be selected to minimize topological and ECM problems. Since DTOA measurements alone are used, the dominant system error source (DF performance) is eliminated. Location errors of the order of 10 meters should be achievable.

The utility of a weapon system employing this approach is that it offers a capability equivalent to passive homing which may be employed against emitters which transmit intermittently. The sole constraint upon weapon time constants is the distance the victim can move once he has ceased transmission. This can be made something on the order of seconds.

SECTION 6

SECTION 6
RECOMMENDATIONS

The technical feasibility of the RTT-1 concept is held adequately verified to warrant serious consideration of its applicability to U.S. Forces signals intelligence collection and emitter targeting needs. The following recommendations constitute prudent, meaningful steps in the overall evaluation of this technique, regarding these applications.

6.1 AN/MSQ-103 AUGMENTATION

An analysis of AN/MSQ-103 characteristics should be performed to determine the expansion in its mission envelope, achievable via the employment of RTT-1 processes. The results of this analysis should include identification of the need for adjunct subsystems and of required operating procedures. ECM vulnerability should be examined.

Field testing, using the present RTT-1 test system, in conjunction with a helicopter-borne repeater, should be conducted. The objective of these tests would be verification of the technical feasibility of this mode of operation.

Field testing, using the present RTT-1 test system, at operational ranges against realistic victim emitters engaged in simulated combat operations should be conducted. The objective of these tests would be the acquisition of design requirement information pertinent to AN/MSQ-103 augmentation operation.

If the results of the preceding analysis/testing warrant, an AN/MSQ-103 system should be made available as an experimental test bed pursuant to concept verification efforts.

6.2 RTT-2 TECHNICAL FEASIBILITY INVESTIGATION

A field test effort, similar in approach and scope to that described in this report, should be conducted to examine the technical feasibility of the RTT-2 concept.

Such a test program would require the use of a three-channel DTOA receiver/processor at the base station, three remotely deployed repeaters and a helicopter-borne guidance package. The latter would provide steering information to the helicopter pilot, permitting guidance to the victim emitter. Existence of the DTOA "line in space" and its manipulability for weapon guidance purposes will be verified.

APPENDIX A

APPENDIX A

ERROR ANALYSES

A.1 σ_η CONSIDERATIONS

From Tables 4-2 and 4-6 we may write:

$$\sigma_{\theta_R} = 0.32° = \sqrt{\left(\frac{0.36}{N}\right)^2 + \sigma_{\theta_{R-M}}^2} \qquad \text{(A-1)}$$

where N is the number of pulses integrated during the measurement and is approximately 100. Solving 4-1, we obtain:

$$\sigma_{\theta_{R-M}} = 0.318° \text{ (100 pulses) or } 3.18° \text{ (1 pulse)} \qquad \text{(A-2)}$$

Similarly, the expression:

$$\sigma_{\theta_V} = 0.089 = \sqrt{\left(\frac{0.00008}{N}\right)^2 + \sigma_{\theta_{V-M}}^2} \qquad \text{(A-3)}$$

can be solved to obtain:

$$\sigma_{\theta_{V-M}} \approx 0.089° \text{ (100 pulses) or } 0.89° \text{ (1 pulse)} \qquad \text{(A-4)}$$

Substituting the results of (A-2) and (A-4) into (4-1) we obtain:

$$\sigma_\eta = 0.36° = \sqrt{\sigma_{sys}^2 + (0.00008)^2 + (0.089)^2 + (0.036)^2 + (0.318)^2} \qquad \text{(A-5)}$$

which may be solved to obtain:

$$\sigma_{sys} = 0.14°$$

The relative magnitude of $\sigma_{\theta_{V-M}}$ and $\sigma_{\theta_{R-M}}$ components, i.e., 0.089° to 0.318° or 3.57, while slightly less than the pertinent beam width ratio (2° to 11.6° or 5.8) are in the correct direction and appear reasonable.

A.2 σ_τ CONSIDERATIONS

(SYS) was examined in the laboratory. For the signal levels encountered and numbers of pulse pairs integrated during the field tests, its values were determined to be 3.7 nsec. (DTOA measurements, 360 pulse pairs integrated) and 4.3 nsec. (TOA measurements, 180 pulse pairs integrated.)

Regarding all other subcomponents, inspection of Table 4-6 indicates that $\frac{S}{N}$ effects contribute a single pulse time measurement error S.D. of 2.2 nsec for the worst-case (repeater to base station) link. During TOA and DTOA measurements in the field, the error contribution from this source is approximately 0.23 and 0.16 nsec, respectively, and is considered negligible in view of the substantial total S.D. values involved. Therefore, all link-related S.D. subcomponent contributions are assumed to be due to multipath effects.

To further simplify analyses to manageable proportions, the following assumptions are made:

$$\sigma_\tau(\text{I-R}) \approx \sigma_\tau(\text{V-BS}) \tag{A-6}$$

since the same base station antenna is operating in conjunction with an omnidirectional pattern (if one accepts that the rear lobes of the AN/PPS-5 antenna exhibit an omnidirectional characteristic), and

$$\sigma_\tau(\text{I-R}) \approx \frac{1}{3.57} \quad \sigma_\tau(\text{R-BS}) \tag{A-7}$$

AD-A076 586 RCA GOVERNMENT SYSTEMS DIV BURLINGTON MA F/G 19/5
RADAR TARGETING TECHNIQUE, REPORT OF METHODS AND RESULTS.(U)
NOV 79 J M ANDERSON , E L WIRTZ DAAB07-78-C-3613
UNCLASSIFIED DELEW-TR-78-3613-F NL

2 OF 2
AD
A076586

END
DATE
FILMED
12-79
DDC

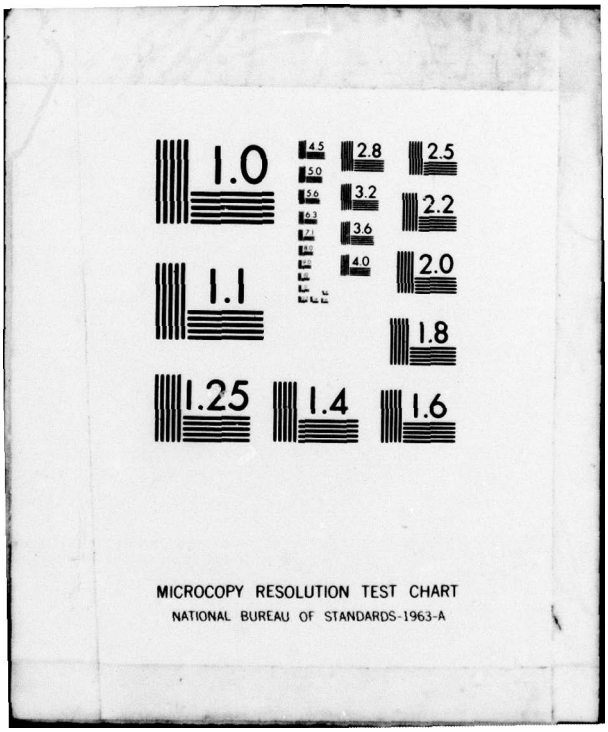
1.0
1.1
1.25
1.4
1.6
1.8
2.0
2.2
2.5
2.8
3.2
3.6
4.0
4.5
5.0
5.6
6.3
MICROCOPY RESOLUTION TEST CHART
NATIONAL BUREAU OF STANDARDS-1963-A

where the 3.57 factor represents the ratio of multipath contributions identified in the DF measurement process relative to these two links.

$$\sigma_\tau(\text{I-BS}) \approx 0 \qquad \text{(A-8)}$$

since the coupling between the interrogator transmitter and the base station was via cable and at a high $\frac{S}{N}$ ratio.

Substituting the preceding results into equation (A-9) we obtain:

$$\sigma_{TOA} = 18.2 = \sqrt{(3.7)^2 + 0 + \left(\frac{\sigma_\tau\ (\text{R-BS})}{3.57}\right)^2 + \sigma_\tau^2\ (\text{R-BS})} \qquad \text{(A-9)}$$

which may be solved to obtain:

$$\sigma_\tau(\text{R-BS}) = 17.02 \quad \text{(180 pulse pairs)} \qquad \text{(A-10)}$$

Using equation (A-12) we obtain:

$$\sigma_\tau(\text{I-R}) = 4.77 \text{ nsec.} \quad \text{(180 pulse pairs)}$$

Substituting these results into equation (A-10) and accounting for the difference in the number of pulse pairs integrated gives:

$$\sigma_{DTOA} = 29.6 \text{ nsec} = \sqrt{(3.7)^2 + (3.4)^2 + \sigma_\tau^2(\text{V-R}) + (12.0)^2}$$

which is solved to obtain:

$$\sigma_\tau(\text{V-R}) = 26.57 \text{ nsec} \quad \text{(360 pulse pairs)} \qquad \text{(A-11)}$$

Combining the preceding results and normalizing the integration to a single pulse pair, produces:

$$\left.\begin{aligned} \sigma_\tau(\text{I-BS}) &= 0 \text{ nsec} \\ \sigma_\tau(\text{I-R}) &= 64.0 \text{ nsec} \\ \sigma_\tau(\text{R-BS}) &= 228.5 \text{ nsec} \\ \sigma_\tau(\text{V-R}) &= 504.2 \text{ nsec} \\ \sigma_\tau(\text{V-BS}) &= 64.0 \text{ nsec} \end{aligned}\right\} \quad \text{one pulse pair}$$

as the S.D. contributions to the time-difference measurement process in the RTT-1 links due to multipath propagation effects.

DISTRIBUTION LIST 5 October 1979

101 Defense Documentation Ctr
ATTN: DDC-TCA
Cameron Station, Bldg 5
002 Alexandria, VA 22314

102 Director
National Security Agency
ATTN: TDL
001** Fort George G. Meade, MD 20755

200 Office of Naval Research
Code 427
001 Arlington, VA 22217

205 Director
Naval Research Laboratory
ATTN: Code 2627
001 Washington, DC 20375

206 Commander
Naval Electronics Lab Ctr
ATTN: Library
001 San Diego, CA 92152

210 Commandant
HQ, US Marine Corps
ATTN: Code LMC
001 Washington, DC 20380

211 Commandant
HQ, US Marine Corps
ATTN: Code INTS
001 Washington, DC 20380

217 Naval Air Systems Command
Code: AIR-5332
001 Washington, DC 20360

301 Rome Air Development Center
ATTN: Documents Library (TILD)
001 Griffis AFB, NY 13441

307 AFGL/SUL
S-29
001 HAFB, MA 01731

*Send 12 copies of UNCLASSIFIED UNLIMITED reports; send 2 copies of LIMITED and CLASSIFIED reports.

311 ASD/ENAD
001 Wright-Patterson AFB, OH 45433

312 HQ, Air Force Electronic Warfare Ctr
ATTN: SURP
001 San Antonio, TX 78243

314 HQ, Air Force Systems Command
ATTN: DLCA
Andrews AFB
001 Washington, DC 20331

403 Commander
Redstone Scientific Info Ctr
ATTN: Chief, Document Section
001 Redstone Arsenal, AL 35809

417 Commander
US Army Intel Ctr & School
ATTN: ATSI-CD-MD (ATTN: Maj. Thorpe)
002 Fort Huachuca, AZ 85613

418 Commander
HQ, Fort Huachuca
ATTN: Tech Reference Div.
001 Fort Huachuca, AZ 85613

419 Commander
US Army Electronic PG
ATTN: STEEP-MT
001 Fort Huachuca, AZ 85613

436 HQDA (DAMO-TCE)
001 Washington, DC 20310

437 Dep for Science & Tech Ofc
Assist Sec Army (R&D)
001 Washington, DC 20310

465 Cdr, US Army Combined Arms
Combat Developments Activity
ATTN: ATCA-COE-I
001 Fort Leavenworth, KS 66027

475 Cdr, Harry Diamonds Labs
ATTN: Library
2800 Powder Mill Road
001 Adelphi, MD 20783

DISTRIBUTION LIST (Continued)

483 Director
US Army Materiel Sys Analysis Acty
ATTN: DRXSY-MP
001 Aberdeen Proving Ground, MD 21005

512 Commander, ARRADCOM
ATTN: DRDAR-LCN-S
001 Dover, NJ 07801

513 Commander, ARRADCOM
ATTN: DRDAR-TSS
001 Dover, NJ 07801

520 Commander
DA Project Manager, FIREFINDER
ATTN: DRCPM-FF
001 Fort Monmouth, NJ 07703

521 Commander
DA, Project Manager, SOTAS
ATTN: DRCPM-STA
001 Fort Monmouth, NJ 07703

531 Cdr, US Army Research Ofc
ATTN: DRXRO-IP
P.O. Box 12211
001 Rsch Triangle Park, NC 27709

532 Cdr, US Army Research Ofc
ATTN: DRXRO-PH (Dr. R. Lontz)
P.O. Box 12211
001 Fort Monroe, VA 23651

554 Commandant
US Army Air Defense
ATTN: ATSA-CD-MD
001 Fort Bliss, TX 79916

556 Commander, HQ, TCATA
Technical Information Ctr
ATTN: Mrs. Ruth Reynolds
001 Fort Hood, TX 76544

563 Commander, DARCOM
ATTN: DRCDE
5001 Eisenhower Ave.
001 Alexandria, VA 22333

565 Cdr, US Army Signals Warfare Lab.
ATTN: DELSW-OS
Vint Hill Farms
001 Warrenton, VA 22186

574 Commander
HQ, TRADOC
ATTN: ATTNG-XD
001 Fort Monroe, VA 23651

575 Commander
US Army Tng & Doctrine Cmd
ATTN: ATCD-TEC
002 Fort Monroe, VA 23651

576 Commander
US Army Tng & Doctrine Cmd
ATTN: ATCD-SIE (Col. W. Gardner)
002 Fort Monroe, VA 23651

577 Commander
US Army Tng & Doctrine Cmd
ATTN: ATCD-TM
001 Fort Monroe, VA 23651

609 Cdr, ERADCOM
ATTN: DRDEL-CG
2800 Powder Mill Road
001 Adelphi, MD 20783

614 Cdr, ERADCOM
ATTN: DRDEL-LL
2800 Powder Mill Road
001 Adelphi, MD 20783

HQ, DARPA
1400 Wilson Blvd.
ATTN: Col. H. Federhen, Rm 1009
002 Arlington, VA 22209

680 Commander, ERADCOM
Fort Monmouth, NJ 07703

5 DELEW-E
1 DELEW-DA (TR Rec File Cy)
1 DELEW-DI
1 DELSD-L
1 DELSD-L-S (UNCL reports only)

DISTRIBUTION LIST (Continued)

Director
National Security Agency
ATTN: R-93 (Col. D. Pins)
002 Ft. George G. Meade, MD 20755

DDR&E
Director International Programs
ATTN: Mr. A. LeBlanc
Rm 3E1082 Pentagon
001 Washington, DC 20310

DDR&E
Director EW & Counter C^3
ATTN: J. Porter
Rm 3E153 Pentagon
001 Washington, DC 20310